INVITED PAPER

An Information Theoretic Framework to Analyze Molecular Communication Systems Based on Statistical Mechanics

This article proposes a mathematical framework to define the main functional blocks of molecular communication theory, supported by general models from chemical kinetics and statistical mechanics.

By Ian F. Akyildiz, *Fellow IEEE*, Massimiliano Pierobon, *Member IEEE*, and Sasitharan Balasubramaniam, *Senior Member IEEE*

ABSTRACT | Over the past 10 years, molecular communication (MC) has established itself as a key transformative paradigm in communication theory. Inspired by chemical communications in biological systems, the focus of this discipline is on the modeling, characterization, and engineering of information transmission through molecule exchange, with immediate applications in biotechnology, medicine, ecology, and defense, among others. Despite a plethora of diverse contributions, which has been published on the subject by the research community, a general framework to study the performance of MC systems is currently missing. This paper aims at filling this gap by providing an analysis of the physical processes underlying MC, along with their information-theoretic underpinnings. In particular, a mathematical framework is proposed to define the main functional blocks in MC, supported by general models from chemical kinetics and statistical mechanics. In this framework, the Langevin equation is utilized as a unifying modeling tool for molecule propagation in MC systems, and as the core of a methodology to determine the information capacity. Diverse MC systems are classified on the basis of the processes underlying molecule propagation, and their contribution in the Langevin equation. The classifications and the systems under each category are as follows: random walk (calcium signaling, neuron communication, and bacterial quorum sensing), drifted random walk (cardiovascular system, microfluidic systems, and pheromone communication), and active transport (molecular motors and bacterial chemotaxis). For each of these categories, a general information capacity expression is derived under simplifying assumptions and subsequently discussed in light of the specific functional blocks of more complex MC systems. Finally, in light of the proposed framework, a roadmap is envisioned for the future of MC as a discipline.

KEYWORDS | Fokker–Planck equation; information capacity; Langevin equation; molecular communication (MC); nanonetworks; Poisson noise; statistical mechanics.

Manuscript received December 2, 2018; revised June 10, 2019; accepted June 27, 2019. Date of current version July 19, 2019. This work was supported in part by the U.S. National Science Foundation under Grant CISE CNS-1763969 and Grant CCF-1816969 and in part by the Science Foundation Ireland through the SFI VistaMilk research centre (16/RC/3835) and CONNECT research centre (13/RC/2077). *(Corresponding author: Massimiliano Pierobon.)*

I. F. Akyildiz is with the Broadband Wireless Networking Laboratory, School of Electrical and Computer Engineering, Georgia Institute of Technology, Atlanta, GA 30332 USA (e-mail: ian@ece.gatech.edu).

M. Pierobon is with the Molecular and Biochemical Telecommunications Laboratory, Department of Computer Science & Engineering, University of Nebraska–Lincoln, Lincoln, NE 68588 USA (e-mail: pierobon@cse.unl.edu).

S. Balasubramaniam is with the Telecommunication Software and Systems Group, Waterford Institute of Technology, X91 P20H Waterford, Ireland, and also with the Department of Electronic and Communication Engineering, Tampere University of Technology, 33720 Tampere, Finland (e-mail: sasib@tssg.org).

Digital Object Identifier 10.1109/JPROC.2019.2927926

I. INTRODUCTION

The genesis of molecular communication (MC) as a discipline stands in the observation of the units of life, i.e., biological cells, where information is

generated, stored, and communicated through molecular processes [1]. Molecules are the common substrates used in cells to represent information, and their chemical reactions and transport mechanisms are the key processes that enable their encoding and propagation. MC aims to build on top of these processes by modeling, characterizing, and engineering communication systems and devices able to tap into a previously uncharted territory, the biochemical, to enable applications where classical communication systems show limitations, i.e., inside the human body and/or directly interacting with biological cells [2]. Current and future MC applications range from the engineering of communication systems between microorganisms [19], to the development and optimization of biomedical devices [12], and the augmentation of the human body functionalities through pervasive intrabody deployment of intercommunicating nanotechnology- and biotechnology-enabled devices, i.e., the Internet of Bio-Nano Things (IoBNT) [3].

Since the birth of this field, the research community, largely driven by communication and networking engineers, as well as computer scientists, has taken different elements from the aforementioned biochemical communication processes and abstracted them into theoretical models to assemble and characterize MC systems. This has led researchers to develop communication channel models based on a wide range of processes for propagating information via molecules, ranging from passive Brownian motion diffusion [17], [18], [60], [83], to the transport, or advection, in fluid currents [10], [12], [76], and to active processes that require a dedicated energy source to move molecules from a transmitter to a receiver [67], [72], [77]. Subsequent contributions have explicitly addressed the estimation or expression of the communication capacity with *ad hoc* studies for some of these MC channels, such as time-slotted ON–OFF keying (OOK) [20], one-shot [21], time-slotted [22], [23], and continuous [24], [25] timing channels, and multiple symbol transmission [26] with perfect transmitter–receiver synchronization for passive Brownian motion and between bacteria colonies [33], time-slotted transmission in the cardiovascular system [11] and continuous transmission in passive Brownian motion [15], [32], and microfluidic systems [74], [75]. Although these contributions have validity for specific MC scenarios, a general information-theoretic framework that captures the peculiarities of an MC channel over classical communication systems is currently missing.

This paper aims at filling the aforementioned research gap by providing a mathematical framework rooted in statistical mechanics to abstract any MC system and determine or estimate the information capacity of their communication channels. As shown in Fig. 1, by stemming from the general formulation of the Langevin equation [9] of a moving nanoscale particle subject to unavoidable thermally driven Brownian forces, we build a general mathematical abstraction of an MC system and its main elements. Subsequently, we derive a methodology to determine

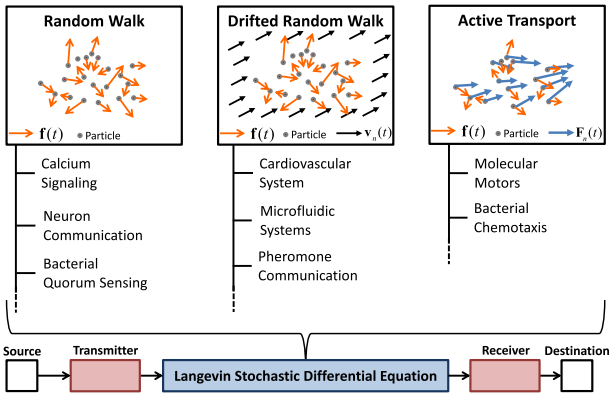

Fig. 1. ***Schematic of the framework proposed in this paper, which stems from the Langevin SDE.***

(or estimate, whenever closed-form analytical solutions are intractable) the MC channel capacity based on the decomposition of the Langevin equation into two contributions, namely, the Fokker–Planck equation [7] and a Poisson process. We classify any MC system on the basis of their representation in terms of the Langevin equation as follows. MC systems based on random walk, such as calcium signaling in cell tissues [39], neuron communication by means of neurotransmitters [49], and bacterial quorum sensing [55], include only the contribution of the Brownian stochastic force $\mathbf{f}$. MC systems based on drifted random walk, such as MC in the cardiovascular system [12], microfluidic systems [74], and pheromone communication between plants [57], include both $\mathbf{f}$ and a drift velocity $\mathbf{v}_n(t)$ as function of the time t for each molecule n, which is independent of the Brownian motion. MC systems based on active transport, such as those based on molecular motors [72] and bacteria chemotaxis [67], include instead a deterministic force $\mathbf{F}_n(t)$ added to $\mathbf{f}$. For each of these categories of MC systems, and based on the aforementioned Langevin equation decomposition, we provide a general information capacity expression under simplifying assumptions and subsequently discuss these results in light of the functional blocks of more specific MC system models, including cases where a closed-form capacity expression cannot be analytically derived.

The rest of this paper is organized as follows. In Section II, we introduce the framework to model and classify MC systems based on the Langevin equation, and we introduce a general methodology to determine their channel capacity. In Sections III–V, we detail general capacity expressions and specific functional block models for MC systems based on a random walk, drifted random walk, and active transport, respectively. Finally, in Section VI, we conclude this paper and discuss the future of MC as a discipline.

II. FRAMEWORK TO ANALYZE MOLECULAR COMMUNICATION SYSTEMS AND THEIR CAPACITY

MC is defined as the transmission, propagation, and reception of information by utilizing molecules and their

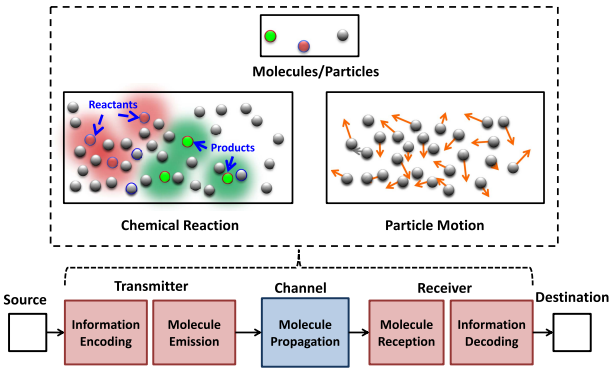

Fig. 2. ***Fundamental processes and functional blocks of an MC system.***

propagation as the medium [1]. **Molecules** are the smallest identifiable units of a substance, a form of matter with specific homogeneous chemical composition and properties. Consequently, a molecule is the smallest unit that still retains information on the substance identity and its ability to take part in chemical reactions. The size of a molecule ranges from that of diatomic hydrogen (0.074 nm), water (0.275 nm), and carbon dioxide (0.232 nm), to the size of a biological macromolecule, such as an average protein (≈2 nm) or a deoxyribonucleic acid (DNA) chain (from 2 nm). In an MC system, their dimensions and the strong forces of the chemical bonds that underlie their structure, and the information they carry, are manipulated by chemical reactions, where molecule composition and structure are rearranged. Chemical reactions are the primary processes underlying the MC transmission and reception. Since a single chemical reaction involves single or a few molecules of one or more (few) substances, an entire MC system has nanoscale precision and can be contained within nanoscale dimensions, and for this reason, MC is identified as a nanocommunication paradigm [2].

To manipulate and propagate information-bearing molecules, the components of an MC system should necessarily be immersed in or include a substance in a fluid state. Brownian motion is the random and independent movement of molecules suspended in a fluid, and it is an unavoidable consequence of the molecule vibrations for a temperature higher than the absolute zero. An MC system is, therefore, subject to Brownian motion as a fundamental stochastic process underlying all its components, and the Brownian motion effects are present in every possible implementation of an MC system.

A. Mathematical Models of Fundamental Processes in MC

With the goal of modeling information propagation in MC, the aforementioned fundamental processes in MC, sketched in Fig. 2, have the following analytical formulation.

1) Molecules of the same substance, which carry information in MC, are considered indistinguishable and equivalent to spherical particles of radius r and mass m, where $r \ll d$, d being the distance between the transmitter and the receiver in an MC system, defined in the following, and s is the particular substance. Consequently, from now on, we will indistinguishably refer to molecules or particles.
2) Chemical reactions are processes that convert one or more input molecules (reactants) into one or more output molecules (products). A reaction j may proceed in forward or reverse directions, which are characterized by forward ($k_{f,j}$) and reverse ($k_{r,j}$) reaction rates, respectively. We assume to have, in general, S chemical substances and M different chemical reactions in their elementary form, i.e., each chemical reaction happens without any intermediate product. They can be expressed as follows:

$$R_{1,j}s_1 + \cdots + R_{n,j}s_S \underset{k_{r,j}}{\overset{k_{f,j}}{\rightleftharpoons}} P_{1,j}s_1 + \cdots + P_{n,j}s_S \quad (1)$$

where $R_{i,j}$ and $P_{i,j}$ are the number of molecules of the substance s_i that participate in a single chemical reaction j expressed in (1) as reactants or products, respectively. This can be mathematically expressed with the following reaction rate equation:

$$V_j = k_{f,j}\prod_{i=1}^{S}[s_i]^{R_{i,j}} - k_{r,j}\prod_{i=1}^{S}[s_i]^{P_{i,j}} \quad (2)$$

where V_j is the rate of the reaction, i.e., the rate of variation in the molecule concentration $[s_j]$ of the substance s_j in number of molecules per unit space. Following classical chemical kinetics, the evolution of the M chemical reactions can be expressed as:

$$\frac{d[s_i]}{dt} = \sum_{j=1}^{M} v_{i.j}V_j, \quad 1 \le i \le S \quad (3)$$

where $v_{i.j} = P_{i,j} - R_{i,j}$ expresses the net change in the concentration $[s_i]$ of the substance s_j due to the jth reaction.
3) Particle motion in a physical system can be analytically formulated according to the Langevin stochastic differential equation (SDE) [9], which states that the location $\mathbf{p}_n(t) = \{p_{n,i}(t)\}_i$ of the particle n at time t along any space dimension i (e.g., one of the 3-D axes X, Y, Z shown in Fig. 3) obeys the following equation:

$$m\frac{d^2\left(\mathbf{p}_n(t) - \mathbf{v}_n(t)t\right)}{dt^2} = \mathbf{F}_n(t) - 6\pi\mu r\frac{d\left(\mathbf{p}_n(t) - \mathbf{v}_n(t)t\right)}{dt} + \mathbf{f}(t) \quad (4)$$

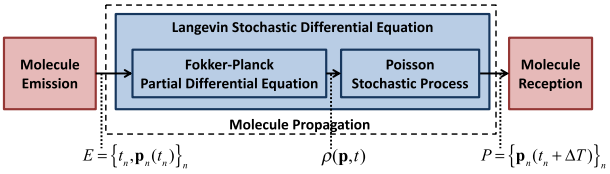

Fig. 3. ***Proposed framework to determine MC channel capacity.***

where m is the molecule mass, $\partial^2(\cdot)/\partial t^2$ and $\partial(\cdot)/\partial t$ are the second and first time derivative operators, respectively, $\mathbf{v}_n(t)$ is a drift velocity of the fluid where the particle n is located, $\mathbf{F}_n(t)$ is a force applied to the particle n independently of its Brownian motion, μ is the viscosity of the fluid, which we assume homogeneous in the propagation space, r is the radius of the particle, and $\mathbf{f}(t)$ is a random process that models the Brownian motion force, whose probability density function is Gaussian and has correlation function $< f_i(t)f_j(t') >$ given by

$$< f_i(t)f_j(t') >= 12\pi\mu r k_B \mathrm{T}\delta_{i,j}\delta(t-t') \tag{5}$$

where $f_i(t)$ is the component of $\mathbf{f}(t)$ in the ith dimension, $< \cdot >$ is the average operator, i and j indicate any of the space dimensions, k_B is Boltzmann's constant, T is the absolute temperature of the fluid, considered homogeneous throughout the space, and $\delta_{i,j}$ is equal to 1 if $i = j$ and zero otherwise, and $\delta(t-t')$ is the Dirac delta function.

B. Functional Blocks of a Molecular Communication System

An MC system [38], defined as a set of natural or engineered components that work together to receive information from a source, encode this information into properties of molecules emitted at a transmitter, propagate the information-bearing molecules through a channel, and reconstruct this information through a **Receiver**, includes the following main functional blocks based on the aforementioned fundamental processes.

1) Information encoding is the modulation of the molecule properties according to the source information $X(t)$, either continuous-time signals or symbols at discrete time instants $t = t_k$, $k \in \mathcal{N}$. These properties can be classified into two main categories, namely, intensive and extensive, following the ways physical systems can be characterized. Intensive properties do not depend on the quantity of the molecules, such as their chemical composition and structure (e.g., protein folding), concentration, density, pressure, or temperature. Extensive properties are instead proportional to the quantity of molecules, such as their number, total mass, occupied volume, enthalpy, or entropy. Some intensive properties can be assigned to a single molecule, e.g., temperature or chemical composition and structure, while others are derived from the ratio between two extensive properties, e.g., concentration or density. Some of these properties are continuous, e.g., concentration (at high molecule number) or temperature, while others are discrete, e.g., molecule number, chemical composition, and structure. The information encoding results in values of these properties as function of the source information $X(t)$. Consequently, the encoding of an intensive property that can be assigned to a single molecule is, here, formalized as

$$\mathrm{Int}_{l,n}(X(t)) = A_l(X(t)) \tag{6}$$

where $A_l(\cdot)$ is the encoding function for the lth intensive property, which determines the intensive property for the nth molecule. The encoding of an extensive property can be formalized as

$$\mathrm{Ext}_{l,m}(X(t)) = b_m(n_l(t)), \quad n_l(t) = C_l(X(t)) \tag{7}$$

where b_m is a proportionality constant for the mth extensive property, $n_l(t)$ is the number of molecules with identical intensive property $A_l(X(t))$ at the transmitter at time t, and $C_l(X(t))$ is a function of the source information $X(t)$. One of the most used intensive properties in MC, namely, the concentration of a substance (characterized by molecules with intensive property l corresponding to a specific chemical composition and structure) can be derived by dividing the number of molecules $n_l(t)$ by their occupied volume $\mathrm{Ext}_{l,m}(X(t))$, where m denotes a specific occupied volume.

2) Molecule emission is the release of information-bearing molecules to the molecule propagation medium. In an MC system, this corresponds to moving the molecules, whose properties compose the encoded signal from inside to outside the space occupied by the transmitter, into the propagation medium. Realistic molecule emission processes include free diffusion, evaporation, dilution, osmosis/dialysis, pressure gradients (e.g., spray), encapsulation, or release from vesicles/reservoirs. The molecule emission results in molecule locations $\mathbf{p}_n(t_n)$ at the boundary $S_\mathbf{T}$ that separates the transmitter from the rest of the space, expressed as

$$\mathbf{p}_n(t_n) \in S_\mathbf{T} \quad \forall t_n, n : N_\mathbf{T}(t_n) > 0, \quad n \in \mathcal{N}_\mathbf{T}(t_n) \tag{8}$$

where $N_\mathbf{T}(t_n) = \sum_l n_l(t_n)$ is the number of molecules emitted at time t_n at the transmitter, and $\mathcal{N}_\mathbf{T}(t)$ is the set containing all the indices of the emitted particles from time 0 to time t

$$\mathcal{N}_\mathbf{T}(t) = \left\{ \int_0^{t'} N_\mathbf{T}(\tau)d\tau \,\middle|\, 0 < t' < t \right\}. \tag{9}$$

3) Molecule propagation is the process whereby the emitted molecules propagate through space from the transmitter location to the receiver location by means of a propagation medium. In an MC system, this propagation is unavoidably affected by the aforementioned Brownian motion, i.e., the Brownian stochastic force **f**, but other processes can be in place to further control the molecule propagation over a completely random walk, represented by the drift velocity $\mathbf{v}_n(t)$ and the force $\mathbf{F}_n(t)$ in (4), both independent of the Brownian motion, where the former results from currents in the fluid, and the latter from other deterministic forces acting on each molecule n. Regardless of the particular underlying process, the molecule propagation can be expressed as the translation of the spatial coordinates from the location $\mathbf{p}_n(t_n)$ at the transmitter to a location $\mathbf{p}_n(t_n + \Delta T)$ at time $t_n + \Delta T$

$$\mathbf{p}_n(t_n) \rightarrow \mathbf{p}_n(t_n + \Delta T), \quad \forall n \in \mathcal{N}_{\mathbf{T}}(t_n) \tag{10}$$

where ΔT is an arbitrary propagation time interval.

4) Molecule reception is the detection of the molecules that propagated to the receiver. The most widespread process for realizing this detection is through chemical reactions between the information-bearing molecules at the receiver and other molecules, i.e., chemical receptors, which can be placed at the receiver boundary or within the receiver space $S_{\mathbf{R}}$. Upon detection, molecules can separate from the chemical receptors and either degrade/be degraded (absorbing receiver) or resume their propagation (nonabsorbing receiver). The set $N_{\mathbf{R}}(t)$ of received molecules at the receiver at time $t > t_n$ is represented as

$$N_{\mathbf{R}}(t) = \{n | \mathbf{p}_n(t) \in S_{\mathbf{R}}\}. \tag{11}$$

5) Information decoding is the demodulation of the properties of the received molecules to obtain an estimate of the source information, which may possibly include noise or errors in the recognition of symbols. Upon effective collision of these molecules, if a chemical reaction takes place, a specific molecule with composition/structure complementary to the chemical reception is recognized as being received. By considering the result of chemical reactions at multiple (different) receptors, in the most general formulation where both intensive and extensive properties are utilized to encode the source information $X(t)$, the reception process output is composed of the estimated values $\widehat{\text{Int}_l}(t)$ and $\widehat{\text{Ext}_m}(t)$ of the intensive and extensive properties of the received molecules. This is expressed as

$$\widehat{X}_{l,n}(t) = A_l^{-1}(\widehat{\text{Int}_l}(t)) \tag{12}$$

$$\widehat{X}_{l,m}(t) = \frac{\widehat{\text{Ext}_m}(t)}{b_m} \tag{13}$$

where $\widehat{X}_{l,n}(t)$ and $\widehat{X}_{l,m}(t)$ are the estimated value of the source information $X(t)$ from the lth intensive property of the received molecule n and from the mth extensive property of molecules with lth intensive property, respectively. $A_l^{-1}(\cdot)$ is the inverse of the encoding function $A_l(\cdot)$ for the lth intensive property, and b_m is the proportionality constant defined in (7). The received information $Y(t)$ is then obtained from $\widehat{X}_{l,n}(t)$ and $\widehat{X}_{l,m}(t)$. The expressions in (12) and (13) are intended to be general and include any possible information encoding scheme on molecule properties. For example, information could be encoded into the sequence of the nucleotides of different DNA strands (intensive properties) and in a different number of copies of each different DNA strand (extensive properties). In the case where the same source information has been encoded both in intensive and extensive properties of the emitted molecules, the received information can be obtained, e.g., through averaging, as follows:

$$Y(t) = \frac{1}{L}\sum_{l=1}^{L}\left(\sum_{n=1}^{N_{\mathbf{R}}(t)}\frac{\widehat{X}_{l,n}(t)}{N_{\mathbf{R}}(t)} + \sum_{m=1}^{M}\frac{\widehat{X}_{l,m}(t)}{M}\right) \tag{14}$$

where we average over the total number L of intensive properties used for encoding the source information $X(t)$. For the intensive properties, we also average over the number of received molecules $N_{\mathbf{R}}(t)$ at time t, while for the intensive properties, we average over the total number of extensive properties M used for encoding.

C. General Principles of Molecular Communication Channel Capacity

The capacity C of an MC channel in [bit/sec] is, here, defined as the maximum rate of transmission between the molecule emission process and the reception process, where this maximum is with respect to all possible probability distributions of the emission process [14]. This is expressed by the general formula from Shannon [6], which defines the capacity as the maximum mutual information $I(E;P)$ between the transmitted signal (emitted molecules) $E = \{t_n, \mathbf{p}_n(t_n)\}_n$, where n is the index of an emitted molecule at time t_n in the set $\mathcal{N}_{\mathbf{T}}(t_n)$, and the received signal (received molecules) $P = \{t_{n_R}, \mathbf{p}_{n_R}(t_{n_R})\}_{n_R}$, where t_{n_R} is the time of reception of one or more molecules, and n_R is the index of a received molecule in the set $N_{\mathbf{R}}(t)$, with respect to the probability density function $f_E(e)$ in all the possible values of the transmitted signal

$$C = \max_{f_E(e)}\{I(E;P)\}. \tag{15}$$

The **mutual information** $I(E;P)$ in [bit/sec] is defined as

$$I(E;P) = H(E) - H(E|P) = H(P) - H(P|E)$$
$$= H(E) + H(P) - H(E,P) \tag{16}$$

where $H(E)$ is the entropy per second of the transmitted signal E [6], $H(E|P)$ is the entropy per second of the transmitted signal E, given the received signal P, $H(P|E)$ is the entropy per second of the received signal P, given the transmitted signal E, and $H(E,P)$ is the joint entropy per second of the transmitted signal E and the received signal P.

The relationship between the transmitted signal E and the propagated signal P in an MC system is expressed, in general, by the aforementioned Langevin SDE (4). According to statistical mechanics, this propagation model can be separated into two distinct contributions, as shown in Fig. 3. The Fokker–Planck equation [7], which is a deterministic partial differential equation (PDE) to compute the probability density of the particles in the propagation space, and a Poisson point process [15], which is a stochastic process that results in the assignment of the particle locations $\mathbf{p}_n$ in the space based on the result of the Fokker–Planck equation. In the following, we detail how to exploit these properties of the molecule propagation process to define general principles to determine the channel capacity in MC systems.

The Fokker–Planck equation describes the evolution of the particle propagation in the space in the variable $\rho(\mathbf{p},t)$, which is the probability distribution of the location of a particle as function of the space coordinates $\mathbf{p} = \{p_i\}$ and time t. The expression of this equation for MC systems accounts for the aforementioned molecule emission as a source of particles at the transmitter. This translates into an additional term, namely, $(1/n)\delta(|\mathbf{p} - \mathbf{p}_n(t_n)|)\delta(t - t_n)$, which corresponds to the contribution of one particle at time t_n and location $\mathbf{p}_n(t_n)$ to the total number n of propagating particles up to time t_n. We make the following assumptions: 1) the diffusing particles have a spherical shape; 2) the diffusing solute particles are in low concentration; 3) their dimension is much larger than the particles of the solvent; and 4) their diffusion is isotropic in the considered space. We express this formulation of the Fokker–Planck equation as follows:

$$\frac{\partial \rho(\mathbf{p},t)}{\partial t} = D\nabla^2\rho(\mathbf{p},t) - \nabla\mathbf{v}(\mathbf{p},t)\rho(\mathbf{p},t)$$
$$+ \sum_{n=1}^{N_{\mathbf{T}}(t)} \frac{1}{n}\delta(|\mathbf{p} - \mathbf{p}_n(t_n)|)\delta(t - t_n) \tag{17}$$

where n is computed from $N_{\mathbf{T}}(t)$ according to (8), $\mathbf{v}(\mathbf{p},t) = (1/m)\int \mathbf{F}(\mathbf{p},t)dt$ [where $\mathbf{F}(\mathbf{p}_n,t) = \mathbf{F}_n(t)$ from (4)], and D is the particle diffusion coefficient, whose expression is as follows:

$$D = \frac{K_b T}{6\pi\mu r} \tag{18}$$

where K_b is Boltzmann's constant, T is the absolute temperature of the system, μ and r are the aforementioned viscosity of the fluid and the particle radius, respectively.

The Poisson point process is expressed through the stochastic process that randomly assigns the location to each transmitted particle according to the particle distribution $\rho(\mathbf{p},t)$ at each time instant t. This process is a spatial Poisson point process where the expected value is the particle distribution $\rho(\mathbf{p},t)$, expressed as follows:

$$\mathbf{p}_n(t) \sim \text{Poiss}\left(\rho(\mathbf{p},t)\right) \quad \forall n \in \mathcal{N}_T(t) \tag{19}$$

where $\mathcal{N}_T(t)$ is given by (9). Although specific MC system implementations will incorporate other stochastic sources, as described in the next sections of this paper, which will impact the performance of the system through noise, we consider the noise generated by the stochastic process in (19) as inevitably present in any MC system described by our general information-theoretic framework.

The cascade of the aforementioned Fokker–Planck equation and the Poisson point process, as illustrated in Fig. 3, defines a Markov chain [6] in the variables E, ρ, and P following the order $E \rightarrow \rho \rightarrow P$. This is justified by the property that E and P are conditionally independent given ρ, which is expressed as follows:

$$f_{E,P|\rho}(e,p) = f_{E|\rho}(e)\, f_{P|\rho}(p) \tag{20}$$

since ρ is a function of E from (6)–(8) and the Fokker–Planck equation in (17), and the distribution of P is a function of ρ from [11]–[14] and [19]. The chain rule applied to the joint entropy of E, ρ, and P states the following [6]:

$$H(E,\rho,P) = H(E,P|\rho) + H(\rho) = H(E|\rho) + H(P|\rho) + H(\rho) \tag{21}$$

since ρ is a deterministic function of E through the information encoding in (7) and (12), molecule emission (8), and molecule propagation (17), then the joint entropy per second of E, ρ, and P is equal to the joint entropy per second of E and P

$$H(E,\rho,P) = H(E,P). \tag{22}$$

By applying (21) and (22) to the third expression in (16), we obtain that the mutual information $I(E;P)$ of the transmitted signal E and the received signal P as the sum of the mutual information of a communication system,

which includes only the Fokker–Planck equation (mutual information $I(E;\rho)$ of the transmitted signal and the particle distribution) and conditional entropy $H(\rho|P)$ of the particle distribution given the received signal

$$\begin{aligned} I(E;P) &= H(E) + H(P) - H(E|\rho) - H(P|\rho) - H(\rho) \\ &= I(E;\rho) + I(P;\rho) - H(\rho) \\ &= H(\rho) - H(\rho|E) + H(\rho) - H(\rho|P) - H(\rho) \\ &= H(\rho) - H(\rho|P) \end{aligned} \tag{23}$$

where we applied the first two definitions of mutual information from (16) and we considered the fact that $H(\rho|E) = 0$ since ρ is completely determined by E (deterministic function of E).

As a consequence of (23), to determine the aforementioned capacity C, it is necessary to analytically express (or estimate) the entropy $H(\rho)$ of the particle distribution and the conditional entropy $H(\rho|P)$ of the particle distribution given the received signal. The former depends exclusively on the Fokker–Planck equation (17), while the latter depends on the Poisson point process in (19). These, in turn, depend on the processes underlying molecule propagation in the particular MC system being considered. In particular, as illustrated in Fig. 1, the aforementioned propagation processes can be classified on the basis of the randomness on the trajectory of the propagating molecules, which impact the particular expression of the Fokker–Planck equation (17). In the following, for each class of MC systems, we present a general information capacity expression under simplifying assumptions and discuss the impact of specific functional block implementations in more realistic MC systems.

III. MOLECULAR COMMUNICATION VIA RANDOM WALK

In MC systems based on random walk, the molecules emitted by the transmitter propagate to the receiver solely by means of Brownian motion. Consequently, the molecule propagation can be modeled by the Langevin equation in (4), where the drift velocity $\mathbf{v}_n(t)$ of the fluid and the Brownian-motion-independent force $\mathbf{F}_n$ are set to zero. MC based on random walk occurs naturally in a number of biological systems, and it is considered the simplest and most widespread molecule propagation process in nature. In the following, we obtain a closed-form expression to compute the capacity of the Brownian motion channel through the aforementioned methodology by defining the functional blocks of a basic abstraction of an MC system via random walk. Subsequently, we provide more specific functional block models of key diffusion-based implementations found in nature, namely, cell calcium signaling, communication through chemical synapses between neurons, and quorum sensing networks of bacteria.

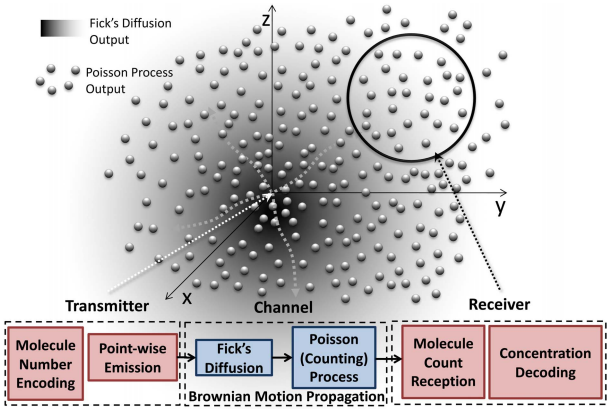

Fig. 4. *Basic abstraction of an MC system based on random walk.*

A. Brownian Motion Channel Capacity

With reference to Fig. 4, we describe the functional blocks of a basic abstraction of an MC system based on random walk.

1) Information Encoding: One single molecule type is modulated in its number $N_{\mathbf{T}}(t)$ at time t proportionally to the source information $X(t)$, expressed as

$$N_{\mathbf{T}}(t) = KX(t), \quad t > 0 \tag{24}$$

which is derived from (6) and (7) by considering $L = 1$, $M = 1$, and $C_1 = K$.

2) Molecule Emission: Molecules are released in a continuous fashion by an ideal point-wise transmitter (size equal to zero) at location $\mathbf{p}_{Tx} = \{p_{x,Tx}, p_{y,Tx}, p_{z,Tx}\}$ in an 3-D space, as shown in Fig. 2. At the time t_n of emission of the nth molecule, its location $\mathbf{p}_n(t_n)$ corresponds to the location of the transmitter $\mathbf{p}_{Tx}$, expressed as

$$\mathbf{p}_n(t_n) = \mathbf{p}_{Tx} \tag{25}$$

where n is a function of $N_{\mathbf{T}}(t)$ according to (8) and (9).

3) Molecule Propagation: Molecules propagate through the Brownian motion in the 3-D space according to (4) where $\mathbf{F}_n = \mathbf{v}_n = 0$. For this basic abstraction model, and to derive analytical expressions to determine the channel capacity, we make the assumption to have a 3-D space with infinite extent in every dimension.

4) Molecule Reception: The receiver detects the particles that are present inside a spherical volume V_R centered at the receiver location and with radius $R_{V_R} \ll d$, where d is the distance between the transmitter and the receiver. This choice makes the results of the Brownian motion channel capacity accounting for the simplest ideal receiver possible (e.g., chemical ligand-binding reception will be further limited by a nonnegligible time of unbinding [16]), where

the number of received molecules $N_{\mathbf{R}}(t)$ is expressed as

$$N_{\mathbf{R}}(t) = \{n|\mathbf{p}_n(t) \in V_R\}\,. \tag{26}$$

5) Information Decoding: This is ideally based on the count of the number of detected molecules expressed as

$$Y(t) = \#N_{\mathbf{R}}(t), \quad t > 0 \tag{27}$$

where $\#$ stands for the cardinality (number of elements) of the set $N_{\mathbf{R}}(t)$ defined in (26).

6) Capacity: As a consequence of the aforementioned functional blocks, the Fokker–Planck equation (17) for this MC system corresponds to the inhomogeneous Fick's second law of diffusion, or diffusion equation [8], expressed as follows:

$$\frac{\partial \rho(\mathbf{p},t)}{\partial t} = D\nabla^2\rho(\mathbf{p},t) + N_{\mathbf{T}}(t)\delta(|\mathbf{p}-\mathbf{p}_{Tx}|), \quad t > 0. \tag{28}$$

As a consequence of the aforementioned molecule reception and information decoding functional blocks, the probability distribution of the output signal $Y(t)$ can be expressed from the aforementioned spatial Poisson point process (19) as follows:

$$Pr_{\{Y(t)|\bar{\rho}(t)\}}(N) = \frac{(\bar{\rho}(t)V_R)^N}{N!}\exp -\bar{\rho}(t)V_R \tag{29}$$

where $\bar{\rho}(t)$ is the average particle distribution inside the receiver spherical volume V_R, for which simplicity is considered equal to the value of the particle distribution at the center $\mathbf{p}_{Rx}$ of V_R, expressed as $\rho(\mathbf{p}_{Rx},t)$, in agreement with the aforementioned assumption on the receiver radius.

The entropy $H(\rho)$ of the particle distribution ρ can be analytically expressed by stemming from the solution to the aforementioned Fick's second law, which is expressed as follows:

$$\rho(\mathbf{p}_{Rx},t) = h_{\text{Diff}}(d,t) * N_{\mathbf{T}}(t) \tag{30}$$

where $d = |\mathbf{p}-\mathbf{p}_{Tx}|$, $*$ is the convolution operation, and $h_{\text{Diff}}(d,t)$ is the impulse response of (28), expressed as follows:

$$h_{\text{Diff}}(d,t) = \frac{e^{-\frac{d^2}{4Dt}}}{(4\pi Dt)^{3/2}}\,. \tag{31}$$

As a consequence of (24), (30), and (31), Fick's second law corresponds to a linear and time-invariant filter applied to the modulated number $N_{\mathbf{T}}(t)$ of emitted molecules. According to the formula to compute entropy loss in linear filters [14], the entropy $H'(\rho)$ per degree of freedom of the particle distribution as expressed in (30) is as follows:

$$H'(\rho) = H'(N_{\mathbf{T}}) + \frac{1}{W}\int_W \log_2|H_{\text{Diff}}(f)|^2\,df \tag{32}$$

where $H'(N_{\mathbf{T}})$ and W are the entropy per degree of freedom and the bandwidth, respectively, of the number of molecules $N_{\mathbf{T}}(t)$, and $H_{\text{Diff}}(f)$ is the Fourier transform of the impulse response in (28). The entropy $H(\rho)$ can be then computed by multiplying the entropy $H'(\rho)$ per degree of freedom by twice the aforementioned bandwidth W. The expression in (32) can be evaluated by considering the following.

1) The modulated number of molecules $N_{\mathbf{T}}(t)$ can be defined as a band-limited ensemble of functions [14] within a bandwidth W, with the following expression:

$$N_{\mathbf{T}}(t) = \sum_{k=0}^{\infty} N_{\mathbf{T}}\left(\frac{k}{2W}\right)\frac{\sin\left[\pi(2Wt-k)\right]}{\pi(2Wt-k)}, \quad k \in \mathbb{N} \tag{33}$$

where the bandwidth W is, here, defined as the maximum frequency contained in the time-continuous signal $N_{\mathbf{T}}(t)$ (24), which corresponds to the modulated number of molecules as function of the time t. The entropy $H'(N_{\mathbf{T}})$ per degree of freedom then equal to the entropy of $N_{\mathbf{T}}(t)$ sampled at time instants $k/(2W)$, which is the first term of the sum in (33).

2) The Fourier transform $H_{\text{Diff}}(f)$ of the impulse response in (28) has the following analytical expression:

$$H_{\text{Diff}}(f) = \frac{e^{-(1-j)\sqrt{\frac{2\pi f}{2D}}d}}{4\pi Dd}. \tag{34}$$

Consequently, the entropy $H(\rho)$ of the particle distribution ρ can be derived from (32) and (34)

$$H(\rho) = 2WH'(N_{\mathbf{T}}) - \frac{4\sqrt{\pi}d}{3\ln 2\sqrt{D}}W^{\frac{3}{2}} - 4W\log_2 4\pi Dd. \tag{35}$$

The conditional entropy $H(\rho|P)$ of the particle distribution given the received signal can be computed from (29) as per time sample of a spatial Poisson counting process with rate parameter equal to ρ. According to [15], this becomes

$$H(\rho|\mathcal{P}) \cong \frac{2}{3}\frac{\mathrm{E}\left[N_{\mathbf{T}}\right]R_{V_R}}{Wd} + \ln\left(\Gamma\left(\frac{2}{3}\frac{\mathrm{E}\left[N_{\mathbf{T}}\right]R_{V_R}}{Wd}\right)\right) + \left(1-\frac{2}{3}\frac{\mathrm{E}\left[N_{\mathbf{T}}\right]R_{V_R}}{Wd}\right)\psi\left(\frac{2}{3}\frac{\mathrm{E}\left[N_{\mathbf{T}}\right]R_{V_R}}{Wd}\right) \tag{36}$$

where $\mathrm{E}\left[N_{\mathbf{T}}\right]$ is the average value of emitted molecules in a time interval equal to $1/(2W)$, W is the bandwidth of the transmitted signal X, $\psi(\cdot)$ is the digamma function,

D is the diffusion coefficient, d is the distance between the transmitter and the receiver, and R_{V_R} is the radius of the spherical receiver volume V_R. The conditional entropy $H(\rho|P)$ is then equal to (36) multiplied by two times the bandwidth W of the modulated number of molecules $N_{\mathbf{T}}(t)$.

The capacity C_{Brown} of the Brownian channel is then obtained by substituting (35) and (36) multiplied by $2W$ into (23), and by maximizing it according to (15) constrained to the **average thermodynamic power** $\bar{P}_{\mathcal{H}}$, defined in [15] as the energy necessary to emit the average number $\mathrm{E}\left[\hat{N}_T\right]$ of particles per time sample $1/(2W)$, divided by the duration of a time sample. The latter is expressed as

$$\bar{P}_{\mathcal{H}} = \frac{3}{2} K_b \mathrm{TE}\left[\hat{n}_T\right] 2W \tag{37}$$

where K_b is Boltzmann's constant, T is the absolute temperature of the system, and W is the bandwidth of the modulated number of molecules $N_{\mathbf{T}}(t)$. The capacity C_{Brown} results in the following expression [15]:

$$\begin{aligned} C_{\text{Brown}} &\cong 2W\left(1+\log_2\frac{\bar{P}_{\mathcal{H}}}{3\,W K_b T}\right) - \frac{4\sqrt{\pi}d}{3\ln 2\sqrt{D}} W^{\frac{3}{2}} \\ &\quad - 4W\log_2 4\pi D d - 2W\frac{2\bar{P}_{\mathcal{H}} R_{V_R}}{9\,W^2\,dK_bT} \\ &\quad - 2W\ln\left(\Gamma\left(\frac{2\bar{P}_{\mathcal{H}} R_{V_R}}{9\,W^2\,dK_bT}\right)\right) \\ &\quad - 2W\left(1-\frac{2\bar{P}_{\mathcal{H}} R_{V_R}}{9\,W^2\,dK_bT}\right)\psi\left(\frac{2\bar{P}_{\mathcal{H}} R_{V_R}}{9W^2 dK_bT}\right) \end{aligned} \tag{38}$$

where $\psi(\cdot)$ is the digamma function, D is the diffusion coefficient, d is the distance between the transmitter and the receiver, and R_{V_R} is the radius of the spherical receiver volume V_R.

B. Calcium Signaling

Calcium signaling is at the basis of biological cell signaling regulation, where it is one form of juxtacrine signaling, which is found in numerous biological regulatory functions in both animals as well as plants [39]. Juxtacrine signaling is a form of close contact cell-to-cell or cell-to-extracellular matrix information exchange. The regulation of the cellular process resulting from the Ca^{2+} signaling can range between millisecond (e.g., protein synthesis and cell division) and minutes as well as hours. This form of signaling can exist in both excitable as well as nonexcitable cells, where the elevated Ca^{2+} concentration can result from triggering of the internal pathways that are due to the ligand-receptor chemical reaction of specific molecules at the cell's membrane. The analysis of Ca^{2+}-based MC is governed by biophysical models, which have been developed through experimental work [40], [41], [45]. Fig. 5

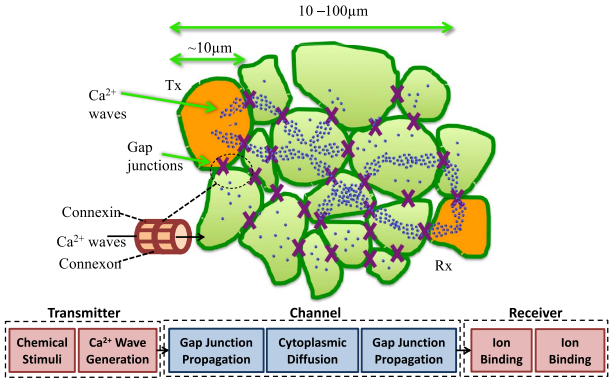

Fig. 5. *Illustration of an MC system based on calcium signaling.*

illustrates the block diagram of a calcium-signaling-based MC system, where communication is established through the diffusion of ions. The calcium propagates through the gap junction to allow the ions to flow between the cells.

1) Information Encoding: The encoding process can be achieved through the elevation of the Ca^{2+} ion concentration $N_{\mathbf{T}}$ from (7) within the cytoplasm of the cell. This is achieved by releasing the Ca^{2+} from the organelles (stores), which is controlled by the intracellular Ca^{2+} signaling pathway, as well as the intake from the extracellular space. The increased concentration of the Ca^{2+} ions within the cytoplasm is dependent on various chemical reaction stimuli, which may include extracellular agonists and intracellular messengers (for nonexcitable cells). One of the most basic models was proposed in [45], and it consists of three types of Ca^{2+} concentration: the cytoplasm (C_{cyt}), the stores within the organelles (C_{str}), and the Ca^{2+} buffer (B). The kinetic model of the type in (3) for these three components is represented as follows:

$$\frac{\partial C_{\text{str}}}{\partial t} = -k_1(h+h_0)(C_{\text{str}}-C_{\text{cyt}}) + V_3\frac{C_{\text{cyt}}^2}{k_4^2+C_{\text{str}}^2} \tag{39}$$

$$\begin{aligned} \frac{\partial C_{\text{cyt}}}{\partial t} &= k_1(h+h_0)(C_{\text{str}}-C_{\text{cyt}}) - V_3\frac{C_{\text{cyt}}^2}{k_4^2+C_{\text{str}}^2} \\ &\quad + k_5(h+h_0)(C_{\text{ext}}-C_{\text{cyt}}) - V_6\frac{C_{\text{cyt}}^2}{k_7^2+C_{\text{str}}^2} \\ &\quad - k_2 C_{\text{cyt}} B + k_2(B_{\text{total}}-B) \end{aligned} \tag{40}$$

$$\frac{\partial B}{\partial t} = -k_2 C_{\text{cyt}} B + k(B_{\text{total}}-B) \tag{41}$$

where k_1 is the rate of Ca^{2+} release and influx for the store, k_2 is the binding constant of Ca^{2+} for the buffers, V_3 is the maximum rate of Ca^{2+} intake to the store, k_4 is the disassociation constant for the store calcium, B_{total} is the total calcium buffer concentration, k_7 is the disassociation constant of the plasma membrane calcium pump (0.6 μm), k_5 is the rate of calcium influx from the external medium (0.000158 sec^{-}1), V_6 is the maximum rate of the plasma membrane calcium pump (1.5 μm/sec), h is the fractional activity of the channels in the store and plasma membrane ($h_0 \leq h \leq 1$), h_0 is the basal fractional

activity of the channels in the store and plasma membrane (0.4), and C_{ext} is the extracellular calcium concentration (1500 μm). Equation (39) reflects the change in the Ca^{2+} in the stored organelles, and this is dependent on the storage release as well as the recovery rate, and the quantity of C_{cyt}; (40) reflects the relationship between the change in C_{cyt}, concentration in the intracellular storage, buffer B in the cytoplasm, extracellular matrix, as well as the release and recovery rate; (41) is the process for the Ca^{2+} binding to the buffer B in the cytoplasm.

Based on (7), the modulated concentration C_{cyt} of Ca^{2+} ion will result in $N_{\mathbf{T}}(t)$ and is represented as

$$N_{\mathbf{T}}(t) = C_{\text{cyt}} X(t), \quad t > 0 \tag{42}$$

where $L = 1$, $M = 1$, and $C_1 = C_{\text{cyt}}$.

2) Molecular Emission: Once the Ca^{2+} concentration is elevated, this results in ion wave generation. A linear channel model can result from the Ca^{2+} concentration once it reaches steady state [39]. The steady state can be achieved when (39)–(41) becomes zero. At the steady-state point, the concentration C_{ssp} is less than the quantity of external Ca^{2+} ions and is represented as follows:

$$C_{\text{ssp}} = k_7 \sqrt{\frac{k_5(h+h_0)C_{\text{ext}}}{V_6 - k_5(h+h_0)C_{\text{ext}}}}. \tag{43}$$

At the same time, the transient response of the Ca^{2+} wave is approximated as follows:

$$C_{\text{cyt}}(t) = C_{\text{cyt}}^{\text{init}} + \left(C_{\text{ssp}} - C_{\text{cyt}}^{\text{init}}\right)(1 - e^{-t\beta}) \tag{44}$$

where $C_{\text{cyt}}^{\text{init}}$ is the initial cytoplasmic calcium concentration, and β is the elevation rate of cytoplasmic calcium [39].

Based on the general molecular emission of MC in (8), the Ca^{2+} ion n released at time t_n will have a location $\mathbf{p}_{Ca^{2+},n}$ that corresponds to the location of the transmitter $\mathbf{p}_{Tx}$ at the center of the cell and is expressed as

$$\mathbf{p}_{Ca^{2+},n}(t_n) = \mathbf{p}_{Tx}. \tag{45}$$

3) Molecular Propagation: The propagation of the wave is established through physical connections between the cells, where the generated waves will travel from the cytoplasm through gap junctions [46]. The gap junctions are composed of two connexons situated on each side of the cell, and they are formed by six proteins called connexins. The probability of the number of open gap junctions s_n out of S_n is modeled as a binomial distribution and is represented as [39]

$$P_r(s_n \text{opens}) = \binom{S_n}{s_n} \zeta_n^{s_n} (1-\zeta_n)^{S_n - s_n}. \tag{46}$$

The opening of the gap junction is dependent on the elevation of the Ca^{2+} concentration. The period for the Ca^{2+} waves to travel through the gap junction is τ_{gap}. The effective gap junctional transitional rate θ_n for cell n, which depends on the level of Ca^{2+}, is represented as

$$\theta_n = \frac{1}{\tau_{\text{gap}}} \frac{P_{Ca}^{(n)}}{D_{Ca}^{(n)}} \tag{47}$$

where P_{Ca} is the permeability of the gap junction and D_{Ca} is the diffusion constant of Ca^{2+} ions. Based on this, the received Ca^{2+} level at the end of the gap junction and the cytoplasm entry of the next cell n is represented as

$$C_{\text{cyt}}^{n}\left(l_{\text{jct}}^{(n)}, \tau_{\text{jct}}^{(n)}\right) = \frac{s_n}{S_n} \theta_n C_{\text{cyt}}^{n-1}\left(l_{\text{jct}}^{(n-1)}, \tau_{\text{jct}}^{(n-1)}\right) \tag{48}$$

where n is the cell receiving the Ca^{2+} emitted from the previous neighboring cell $n-1$. l_{jct} is the gap junction position, and τ_{jct} is the time instant Ca^{2+} travels through the gap junction between cells $n-1$ and n. Once the Ca^{2+} wave enters the cytoplasm of cell $n-1$, it will propagate through diffusion. The modified Fick's law for this diffusion is represented as

$$C_{\text{cyt}}^{n}(x,t) = \frac{1}{\sqrt{4\pi D_{Ca}^{(n)} \tau_{\text{cyt}}^{(n)}}} e^{-(x^2/4D_{Ca}\tau_{\text{cyt}}^{(n)})} \tag{49}$$

where x is the 1-D distance that is perpendicular to the gap junction entry into the cytoplasm, and τ_{cyt} is the delay propagation of Ca^{2+} in the cytoplasm. This is represented as the inhomogeneous Fick's second law of diffusion as in (28), with boundary conditions that are defined by the cell's membrane. The boundary conditions of the cell membrane ensure that the finite space contains the oscillations of the Ca^{2+} ions within the cytoplasm. We also assume that interference between these oscillations and other components of the cell is negligible. From (28), ρ is the distribution of $C_{\text{cyt}}^{n}(x,t)$, $\mathbf{p}$ is the location of the ions within the cell, D is the diffusion coefficient $D_{Ca}^{(n)}$, and $N_{\mathbf{T}}$ is the number of Ca^{2+} ions as in (42).

Although the models that have been presented are between two cells, the channel can be extended to multiple cells as the Ca^{2+} propagates through the tissue.

4) Molecular Reception: The Ca^{2+} that propagates into each cell will be sensed, and the concentration changes will invoke the subsequent wave generation. The regeneration of the Ca^{2+} ion waves as it passes from one cell to the next is based on the internal Ca^{2+}-induced Ca^{2+} release process, and this will depend on the increase in Ca^{2+} concentration that has been received. Once the number $N_{\mathbf{R}}(t)$ (11) of received Ca^{2+} ions binds to the organelles of the receiving cell, this will invoke the intracellular Ca^{2+} signaling pathway to restart the generation of Ca^{2+} waves for the next cell.

5) Information Decoding: Depending on the approach taken for encoding the information into the Ca^{2+} ion concentration, the decoding process will sample the waves that are received in the cytoplasm. In the case of amplitude modulation, the receiver will sample the peak as well as the duration of the arrived Ca^{2+} waves.

6) Capacity: Given the highly stochastic behavior of calcium signaling, a closed-form expression for calcium signaling has not been developed. In [39], the gain and delay of Ca^{2+} waves traveling through a 1-D array of cells were proposed. This was developed from extracting the linear channel behavior of Ca^{2+} waves that are generated from the cells, as well as a stochastic gap junction model in (46). A capacity expression was developed in [43] for a 1-D array of cells, using empirical measurements for the entropy of the received Ca^{2+} wave that was used to determine the mutual information. The same approach was developed in [44] for a channel model of a multidimensional array of cells representing a tissue. The analysis considered the biophysical properties of three different types of cells (e.g., smooth muscle cells, epithelial, and astrocytes), and how these impact on the Ca^{2+} wave propagation. The analysis also considered the reflective behavior of the Ca^{2+} waves due to the boundary conditions of the tissue. In [62], a channel model was also developed between the two cardiomyocyte cells, based on the electrochemical signaling that influences the Ca^{2+} propagation. The significance of this channel model was the introduction of an electrochemical model for Ca^{2+} signals that are generated from excitable cells. The mutual information was developed based on the OOK modulation of Ca^{2+} waves, out of which the capacity was obtained.

An open issue for the future is the development of a closed-form expression for the capacity model. This closed-form expression must include the impact of interactions between organelles (e.g., endoplasmic reticulum and mitochondria) that contribute toward Ca^{2+} generation. This model could then be utilized to understand the impact of abnormalities between the intracellular to intercellular signaling, and how disease can result from this.

C. Neuron Communications

One of the most complex regulatory systems within the human body is the nervous system. The nervous system mimics an information highway that interconnects a number of different organs as well as various physiological subsystems to the brain. This information highway controls and maintains homeostatic equilibrium while ensuring adaptations as an organism faces varying environmental changes [47]. This highly complex system communicates through electrical stimulation based on a compound action potential (AP). At a single-cell level, the nervous system as well as the brain are constructed from neurons, which communicate through electrochemical impulse signals known as AP spikes. Through the highly complex interconnection of neurons, the brain is able to process information, create

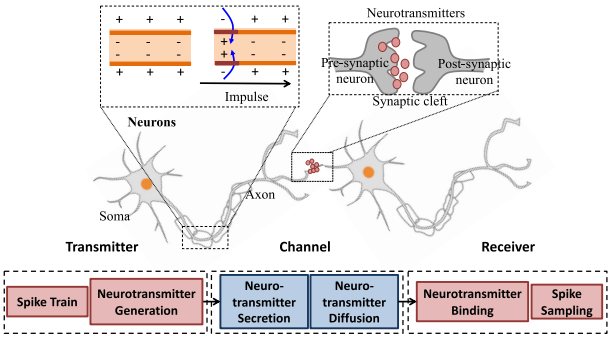

Fig. 6. ***Sketch of an MC system based on neuron communications.***

actions through the control of muscles, store information for both short- and long-term memory, as well as controlling emotions, sensations, and perception.

1) Information Encoding: The discrete impulse signal, or the AP, is established through both electrical and chemical impulses that occur in parallel. The electrical impulses, i.e., electrical spikes, travel through the neuron, while the chemical impulses propagate on the surface of the cell. The information that is conveyed between the neurons depends on the frequency of the electrical spikes that travel through the cell. As the electrical spike propagates down the axon, this will result in the chemical impulse that depolarizes and repolarizes the chemical balance of the neuron. Fig. 6 illustrates this process. Before the electrical spike propagates down the axon, there is a chemical balance in the quantity of ions both inside and outside the neuron. At rest, there is more potassium ions (K^+) and negative ions ($-$ve) inside the axon, while higher sodium ions (Na^+) and positive ions ($+$ve) outside. As the impulse propagates down the axon, the depolarization process starts, where the K^+ ions will diffuse outwards from the axon, and the Na^+ ions will diffuse in the opposite direction into the axon. After a short period, the repolarization process starts, and this will result in the reverse process. This sequence will continue until the impulse arrives at the terminal synapse. Since the information traveling through the neuron is dependent on the type of stimulated and train of spikes, the encoding process can be established through the variations in the electrical spike train. The train of spikes carries the information to be projected onto the subsequent target neuron, and this is considered as neural codes that are transmitted through the network. The train of spikes that carry the codes is not only affected by the types of neurons but also by the synaptic connections to other neurons, which can be either inhibitory or excitatory. This is one of the elements of how physical changes in the environment due to sensory changes (e.g., touch and hearing) can be processed in the brain as unique information.

As the spike travels down the axon, this will lead to the neuron–neuron communication process. Although electrical synapse can also occur for neuron-to-neuron

communication, where AP is transferred through the gap junctions of the cells, in this paper, we only consider the chemical synapse through the diffusion of neurotransmitters (note that the chemical synapse is different from the chemical signaling that occurs only along the axon of the neuron). Once the spike arrives at the synaptic terminal, the vesicles containing the neurotransmitters will bind to the terminal membrane to release the neurotransmitters into the synaptic cleft, by following a stochastic process. A model for this process has been proposed in [61]. The model considers the vesicles are packed in a pool, and when a spike arrives at the synaptic terminal, a single vesicle will be released. Two types of vesicle release process are discussed, which are evoked and spontaneous. For the evoked release, given that the spike time begins at t_0 and the duration Δt_s, the release occurs in the time interval $[t_0, t_0 + \Delta t_s]$. During this period, the probability of evoked release for $N_{\mathbf{T}}$ vesicles within the pool is $1-\exp(-N_{\mathbf{T}}\alpha_v \Delta t)$ for $\Delta t \leq \Delta t_s$ and $1 - \exp(-N_{\mathbf{T}}\alpha_v \Delta t_s)$ for $\Delta t > \Delta t_s$ (this is for a release rate α_s). We do not consider the stochastic production of $N_{\mathbf{T}}$ and assume a fixed quantity of production as well as secretion, because this is highly dependent on the type of cells as well as pattern of AP signals. In the case of spontaneous release, the waiting time before secretion is approximately 8 min, and for this reason, the probability of release for N_v vesicles within the pool during Δt is $1 - \exp(N_v \Delta t/480))$. Based on a maximum vesicle capacity N_v in the pool, the release in ith time slot (time slot is Δt larger than the refractory period) is determined by the probability $F(N_v)$, expressed as follows:

$$F_i(N_v) = 1 - \left[\exp(-N_v \alpha_v \Delta t_s) p_s + \exp\left(-\frac{N_v \Delta t}{480}\right)(1 - p_s)\right] \tag{50}$$

where p_s is the probability of a spike arrival at the ith time slot, which is a Poisson process with rate equal to the source information $X(t)$, with the following expression:

$$p_s = 1 - \exp\{-X(t)\Delta t\}. \tag{51}$$

The model also considers one vesicle vacancy replenishment $G(\tau_D, \Delta t)$, where τ_D is the mean recovery time for one vacancy after Δt, and is modeled as a Poisson process ($G(\tau_D, \Delta t) = 1 - \exp - \tau_D^{-1}\Delta t)$). After Δt, the vesicle recovery is governed by a binomial distribution ($B(N_{\text{MAX}} - N, G(\tau_D, \Delta t))$) [61].

2) Molecular Emission: When the released vesicle binds onto the membrane, it will secrete $N_{\mathbf{T}}(t)$ neurotransmitters at the same time t. We assume the neurotransmitters release to be point-wise, as defined in (8). This is expressed as in (8), where $\mathbf{p}_n = (p_{n,x}, p_{n,y}, p_{n,z})$ and $S_{\mathbf{T}}$ corresponds to points in the membrane surface of the neuron facing the synaptic cleft.

3) Molecular Propagation: These neurotransmitters will propagate through diffusion in the synaptic cleft (the distance of the synaptic cleft is approximately 20 nm). The region of diffusion for the neurotransmitters is a confined space. This means that at an initial stage, a number of neurotransmitters will bind to the postsynaptic neuron, while a short period later, a different number will arrive to bind. This is modeled in [60] with the following expression:

$$\rho(N_{\mathbf{T}}, \mathbf{p}, t) = \frac{N_{\mathbf{T}}}{(\sqrt{4\pi D t})^3} e^{\frac{-(p_x - p_{n,x})^2 - (p_y - p_{n,y})^2}{4Dt}} \left\{ \sum_{k=-\infty}^{-1} (2 - P_u)(1 - P_u)^{-k+1} e^{\frac{-(p_z - (2k+1)H)^2}{4Dt}} + \sum_{k=0}^{\infty} (2 - P_u)(1 - P_u)^{k} e^{\frac{-(p_z - (2k+1)H)^2}{4Dt}} \right\} \tag{52}$$

where ρ is the probability density of neurotransmitters at location $\mathbf{p} = (p_x, p_y, p_z)$ in the synaptic cleft, P_u represents the uptake probability of the neurotransmitters (when $P_u = 0$, none of the neurotransmitters have reached the postsynaptic neuron for uptake, while $P_u = 1$, means all have reached the target within a specified time), H is the length of presynaptic cleft along the z-axis, and D is the diffusion coefficient of the neurotransmitters. The location $\mathbf{p}_n$ of each neurotransmitter is based on a Poisson point process as in (19).

4) Molecular Reception: As these neurotransmitters diffuse and arrive at the postsynaptic neuron, they will bind onto the receptors forming a ligand-receptor complex. According to [61], the binding probability is based on an expected neurotransmitter flux that will bind to vacant receptors during the sampling time t. This means that as the neurotransmitters arrive at the postsynaptic neuron, the number of vacant receptors will also reduce. This will also reduce the binding probability as the sampling time increases. Therefore, at the kth sampling time, the binding probability will be represented as

$$P_b(k\Delta t) = a(k\Delta t)[1 - (1 - P_e(k\Delta t)^{N(k\Delta t)})] \tag{53}$$

where the probability P_e of finding the neurotransmitters inside the effective volume V_e is as follows:

$$P_e(t) = \iiint_{V_e} \rho(N_{\mathbf{T}}, \mathbf{p}, t) d\mathbf{p} \tag{54}$$

where Δt is the duration of the sampling period, and a is the availability of a receptor $[0, 1]$. The probability of the neurotransmitters within the volume space of the synaptic cleft will be the basis of the prediction of the quantity of neurotransmitters that will bind to the receptors of the postsynaptic neuron. This results in a relationship between the binding process and the patterns of spike

trains generated to carry the information between the neurons. a is also adjusted for the next step and expressed as follows:

$$a((k+1)\Delta t) = a(k\Delta t) - P_b(k\Delta t). \tag{55}$$

Therefore, the expected number $N_{\mathbf{R}}$ of neurotransmitters bindings in each sampling period is the summation of binding probabilities of all the receptors and is represented as follows:

$$N_R(k\Delta t) = M_0 P_b(k\Delta t) \tag{56}$$

where M_0 is the number of receptors at the receiver.

5) Information Decoding: When sufficient neurotransmitters bind onto the receptors of the postsynaptic neuron, it will invoke an impulse that will again travel along the neuron, which will open a channel that allows the positive ions to flow into the cell, starting another impulse, which was described in the information encoding.

6) Capacity: A physical channel model was developed in [49] for two neurons, considering the mutual information of the AP and the diffusion of neurotransmitters in the synaptic cleft. In [51], an upper bound information capacity model was developed for both bipartite and tripartite neural connections using results from optical Poisson channels. The Poisson channel model was used to represent the impulse of AP that is generated from the presynaptic neurons, and how this varies depending on the feedback control from the astrocytes. A multiple access model for neural connections was also developed in [48] based on a sequence of spike timings from the presynaptic neurons. This is based on multiple presynaptic neurons that form connections to the postsynaptic neuron and specifically on the capacity that is impacted from the variations in the AP. The limitations in all these capacity models are that there are no closed-form solutions proposed. This is an open research problem that needs to be investigated for the future. The closed-form expression should also consider the impact of different types of biophysical properties of the neurons, and how this impacts the capacity. This can lead to applications of neuron communication models that can be applied to understanding neuronal disease, such as the correlation between impairments of the signaling process and changes in the AP signaling sequences. An extension toward neuronal networks will also need to be investigated, by understanding how the MC varies as signals propagate through heterogeneous neurons (e.g., pyramidal and fusiform) in the network.

D. Bacterial Quorum Sensing

Besides the communication process through the transfer of DNA, bacteria also have another form of natural communication that uses molecules. This communication is based on the simple secretion of molecules, and this could be cooperative between all the bacteria in the vicinity. This form of communication is found in both Gram-negative and Gram-positive bacteria. One bacterial functionality that results from this simple communication is known as quorum sensing, where the bacteria communicates through molecules known as autoinducers and results in synchronized gene expression of the bacterial population (the autoinducers are known as messenger molecules). This communication is ineffective when the bacterium is on its own; however, as a population, this leads to numerous powerful functionalities, and hence the name "quorum." A number of diverse physiological activities can emerge from quorum sensing, and examples include biofilm formation, antibiotic production, and bioluminescence. Fig. 7 illustrates an MC system that is based on the bacterial quorum sensing communication process.

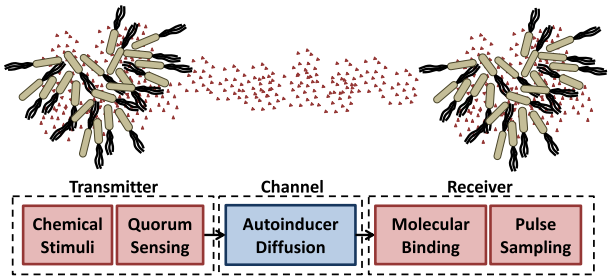

Fig. 7. *Scheme of an MC system based on bacterial quorum sensing.*

1) Information Encoding: The encoding process can be achieved by stimulating the bacterial population with an external chemical signal, in order to produce autoinducers. For example, in [56], signaling molecule N-(3-Oxyhexanoyl)-L-homoserine lactone, or C6-HSL, was injected into engineered *E. coli* bacteria and in response, this resulted in the cells activating a genetic program to produce green fluorescent protein (GFP). In this simple setup, OOK was achieved, where the application of C6-HSL produced a pulse that represents a single bit. Another example is the generation of pulse-amplitude modulation (PAM) using a similar excitation approach [55].

Molecule emissions by the bacteria are initiated from stimuli excitation, either through the influence of external chemicals applied to the population such as C6-HSL described above or initiated from a bacterium within the quorum, which will result in a chain reaction of other cells within the vicinity to produce the molecules collectively. In this paper, we will only focus on the first case, where external stimuli are applied to the bacterial population. The assumption for this case is that external stimuli, which correspond to administrations of a chemical agent, can be assumed evenly distributed throughout the population, resulting in all bacteria equally producing the autoinducer molecules to be emitted.

The following equations define the collective production of molecules by the bacterial population [64], where the source information $X(t)$ is the basis for the production of autoinducers $A(t)$, expressed through a chemical kinetic model (3) as follows:

$$\frac{dA(t)}{dt} = c_A + \frac{k_A C(t)}{K_A + C(t)} - k_0 A(t) - k_1 R(t) A(t) + k_2 RA(t) - p_{\text{out}} A(t) + p_{\text{in}} E(t) \quad (57)$$

$$\frac{dR(t)}{dt} = c_R + \frac{k_R C(t)}{K_R + C(t)} - k_3 A(t) - k_1 R(t) A(t) + k_2 RA(t) \quad (58)$$

$$\frac{dRA(t)}{dt} = k_1 R(t) A(t) - k_2 RA(t) - 2k_4 RA(t)^2 + 2k_5 C(t) \quad (59)$$

$$\frac{dc(t)}{dt} = k_4 RA(t)^2 + k_5 C(t) \quad (60)$$

$$\frac{dE(t)}{dt} = (p_{\text{out}} A(t) - p_{\text{in}} E(t)) - DA(t). \quad (61)$$

Equation (57) is the production rate of internal autoinducer $A_T(t)$ within the bacterium, and this is used to further produce more molecules; (58) is the production rate of receptors inside the bacterium, which will bind to the internal autoinducers to transform the complex into a receptor-bound autoinducer (RA) monomer; (59) is the production rate of RA monomers, and this depends on the number of autoinducers (A), receptors (R), as well as the dimers (C); (60) is the production rate of the RA dimers. A dimer is an association of two monomers, and in this case, it is the association of two RA complex. Equation (61) is the production rate of the autoinducer secreted from each bacterium membrane, which will freely diffuse into the environment and result in a spatially homogeneous concentration.

2) Molecular Emission: A concentration of autoinducers $A(t)$ is released collectively from the bacterial population, as defined in (8), where S_T is now the volume of the colony.

3) Molecular Propagation: The autoinducers concentration $A(t)$ emitted by the transmitter bacteria will diffuse into the environment. The diffusion process will follow the inhomogenous second Fick's law similar to (28), this time expressed as:

$$\frac{\partial \rho(\mathbf{p}, t)}{\partial t} = D\nabla^2 \rho(\mathbf{p}, t) + \sum_{n=1}^{A(t)} \frac{1}{n} \delta(|\mathbf{p} - \mathbf{p}_n(t_n)|) \delta(t - t_n) \quad (62)$$

where $\rho(\mathbf{p}, t)$ is the distribution of autoinducers at location $\mathbf{p}$ and time t.

4) Molecular Reception: The bacteria receives the autoinducer molecules, which leads to an internal signal pathway process in response. The probability of the molecules binding to a bacterium's ith receptors is represented as a chemical kinetic model (3) and expressed as follows [63]:

$$\frac{dp_i}{dt} = -\kappa p_i + \rho(\mathbf{p}, t)|_{\mathbf{p} \in S_{R_i}} \gamma (1 - p_i) \quad (63)$$

where $\rho(\mathbf{p}, t)|_{\mathbf{p} \in S_{R_i}}$ is the distribution of autoinducers within the receiver ith bacterium volume S_R, γ is the input gain, and κ is the rate at which the molecules that have bound to the receptor will detach from the receptors.

There is also randomness in the binding process of the molecules to the receptors of the bacterium. According to [59], for each bacterium i, the number of activated receptors X_i is a Binomial random variable with parameters (M_o, p_i), where M_o is the number of receptors and p is the probability of binding for the ith bacterium as defined in (63). Based on this, $N_{\mathbf{R}}$ will be the total number of activated receptors, where $N_{\mathbf{R}} = \sum_{i=1}^{M_o} X_i$. However, a reporter mechanism is required in response to receiving the molecules. This could be through the expression of GFP, where the fluorescence proteins will reflect a green light when illuminated by an ultraviolet light that can be detected through a photodetector or even imaging technologies on board of a microscope.

5) Information Decoding: Depending on the reporting mechanism taken, the approach for decoding will be through sampling. In the event of fluorescence using GFP, sampling can be performed on the intensity pulse that is generated. Sampling efficiency for GFP generated pulse was investigated in [55] based on the peak value, the total response duration, the ramp-up slope, as well as the ramp-down slope.

6) Capacity: Although there has not been any closed-form expression for the capacity of bacterial quorum sensing, there has been a number of channel models developed based on numerical expressions using mutual information. In [55] and [56], an experimental MC model was developed between two populations of bacteria that communicate through the diffusion of autoinducers, which was part of the National Science Foundation MoNaCo project [58]. In [56], the capacity was defined based on the mutual information in communication-by-silence of bacterial quorum sensing. Communication-by-silence was originally proposed for noisy wireless channels, and this suits the high latency propagation of molecules for bacterial quorum sensing. The capacity model was based on the delay between two-pulses representing the start and stop bits that are transmitted, where the counting process between the delay represents the information. In [59], a mutual information expression for capacity was defined for multihop bacterial network using quorum sensing. The expression considers the intracellular to intercellular signaling that produces the diffused molecules between separate bacterial populations. The next evolutionary step that is required is a closed-form solution for the bacterial quorum sensing. The closed-form model should

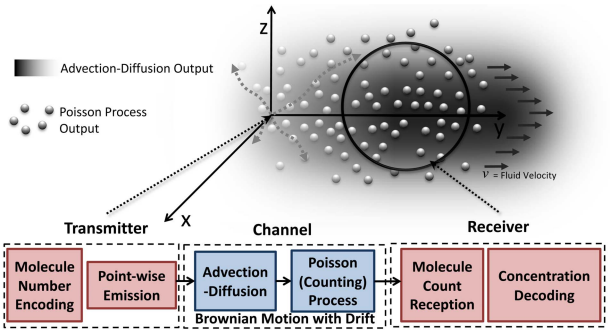

Fig. 8. ***Basic abstraction of an MC system based on drifted random walk.***

integrate the types of bacteria as well as molecules that are produced, and the interactions between different bacteria species, which, to date, have not been investigated in the MC community. Applications can result from the communication process of the bacterial quorum sensing, such as the impact of attacks from different species that can be detected from variations of the communication performance. An example application is in [54], where a synchronization between nanomachines was proposed using the quorum sensing.

IV. MOLECULAR COMMUNICATION VIA DRIFTED RANDOM WALK

In MC systems based on drifted random walk, the molecules emitted by the transmitter not only propagate via Brownian motion but their locations change with a velocity $\mathbf{v}_n(t)$ independent of the Brownian motion or the viscosity of the fluid. Consequently, this propagation is modeled by the Langevin equation in (4) with Brownian-motion-independent force $\mathbf{F}_n(t)$ set to zero. In the following, we revise the Brownian motion capacity expressed in Section III-A through the definition of a basic abstraction of an MC system via based on Brownian motion with drift. Subsequently, we exemplify more realistic functional block models of system based on drifted random walk, which have been studied in recent years, namely, MC based on the cardiovascular system or microfluidic platforms and pheromone communication between plants.

A. Capacity of the Brownian Motion Channel With Drift

The basic abstraction of an MC system via Brownian motion with drift is shown in Fig. 8. In the following, we describe the differences in the channel model with respect to the Brownian motion channel detailed in Section III-A.

1) Molecule Propagation: Molecules propagate by summing the Brownian motion components with a constant and homogeneous drift velocity $\mathbf{v} = \{v_x, v_y, v_z\}$ in the 3-D space according to (4) where $\mathbf{F}_n(t) = 0$, and $\mathbf{v}_n(t)$ is constant and equal to $\mathbf{v}$ for every particle n. As in Section III-A, we make the assumption to have a 3-D space with infinite extent in every dimension.

2) Capacity: As a consequence of the aforementioned molecule propagation, the Fokker–Planck equation (17) for this MC system corresponds to the inhomogeneous Smoluchowski equation, or advection–diffusion equation [7], expressed as follows:

$$\frac{\partial \rho(\mathbf{p},t)}{\partial t} = D\nabla^2 \rho(\mathbf{p},t) - \mathbf{v}\nabla\rho(\mathbf{p},t) + N_{\mathbf{T}}(t)\delta(|\mathbf{p}-\mathbf{p}_{Tx}|). \tag{64}$$

Since this MC system utilizes the same functional blocks for the molecule reception and information decoding as those described in Section III-A, the Poisson point process (19) again becomes a Poisson counting process as expressed in (29).

The entropy $H(\rho)$ of the particle distribution ρ can be analytically expressed similar to Section III-A, but this time based on (64), which is expressed as follows:

$$\rho(\mathbf{p}_{Rx},t) = h_{\text{Adv}}(\mathbf{p}_{Tx},\mathbf{p}_{Rx},t) * N_{\mathbf{T}}(t) \tag{65}$$

where $h_{\text{Adv}}(\mathbf{p}_{Tx},\mathbf{p}_{Rx},t)$ is the impulse response of (64), expressed as follows:

$$h_{\text{Adv}}(\mathbf{p}_{Tx},\mathbf{p}_{Rx},t) = \frac{e^{-\frac{|\mathbf{p}_{Rx}-\mathbf{p}_{Tx}-\mathbf{v}t|^2}{4Dt}}}{(4\pi Dt)^{3/2}}. \tag{66}$$

As for Fick's second law in Section III-A, also the advection–diffusion described in (30), (64), and (66) corresponds to a linear and time-invariant filter applied to the modulated number $N_{\mathbf{T}}(t)$ of emitted molecules. Consequently, we can apply the formula in (32) where the term $H_{\text{Diff}}(f)$ is substituted with $H_{\text{Adv}}(f)$, which is the Fourier transform of the impulse response in (66). The latter does not have analytical solution such as (31), and the following expression has to be solved numerically:

$$H_{\text{Adv}}(f) = \int h_{\text{Adv}}(\mathbf{p}_{Tx},\mathbf{p}_{Rx},t))e^{-j2\pi ft}dt. \tag{67}$$

Consequently, the entropy $H(\rho)$ of the particle distribution ρ can be expressed as follows:

$$H(\rho) = 2WH'(N_{\mathbf{T}}) + \int_W \log_2 |H_{\text{Adv}}(f)|^2 \, df. \tag{68}$$

The conditional entropy $H(\rho|P)$ of the particle distribution given the received signal can be derived similar to Section III-A, and expressed as in (36)

The capacity C_{DBrown} of the Brownian channel with drift is then obtained by substituting (36) and (68) multiplied by $2W$ into (23), and by maximizing it according to

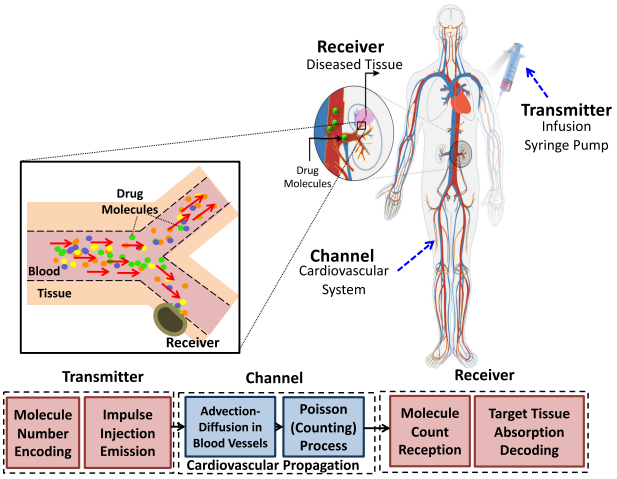

Fig. 9. ***MC functional blocks based on the cardiovascular system.***

(15) constrained to the average thermodynamic power $\bar{P}_{\mathcal{H}}$ expressed in (37). The maximum value expression can be obtained similarly as in [15] even without an analytical expression for $H_{\text{Diff}}(f)$, since the latter does not depend on the probability distribution of the modulated number of molecules $N_{\mathbf{T}}(t)$. The capacity C_{DBrown} results in the following expression [15]:

$$\begin{aligned} C_{\text{DBrown}} &\cong 2W\left(1+\log_2\frac{\bar{P}_{\mathcal{H}}}{3\,W K_b T}\right) \\ &\quad + \int_W \log_2\left|H_{\text{Adv}}(f)\right|^2\, df - 2W\frac{2\bar{P}_{\mathcal{H}}R_{V_R}}{9\,W^2\,dK_bT} \\ &\quad - 2W\ln\left(\Gamma\left(\frac{2\bar{P}_{\mathcal{H}}R_{V_R}}{9\,W^2\,dK_bT}\right)\right) \\ &\quad - 2W\left(1-\frac{2\bar{P}_{\mathcal{H}}R_{V_R}}{9\,W^2\,dK_bT}\right)\psi\left(\frac{2\bar{P}_{\mathcal{H}}R_{V_R}}{9W^2dK_bT}\right) \end{aligned} \tag{69}$$

where $\psi(\cdot)$ is the digamma function, D is the diffusion coefficient, d is the distance between the transmitter and the receiver, and R_{V_R} is the radius of the spherical receiver volume V_R.

B. Cardiovascular System

The cardiovascular system is a molecule propagation network in the human body composed of the heart, the blood, and the blood vessels, where the heart pumps the blood through the blood vessels, resulting into a drift of the molecules that are subject to Brownian motion within the blood. An MC system has been modeled around the cardiovascular system as an MC channel, with the final goal of studying the body distribution of drug molecules within particulate drug delivery systems (PDDSs) [10]–[12], and this is illustrated in Fig. 9. In such systems, drug molecules are injected into a blood vessel at a specific location of the cardiovascular system, they propagate through drifted random walk along the blood vessels, while they distribute through bifurcations to their branches, until reaching the diseased location of the body in need of the drug, where the drug molecules are absorbed by the tissues. Such a study demonstrates a direct application of MC theory to personalized nanomedicine, where the final goal is to provide a methodology to optimize the PDDSs parameters, such as the injection location and time evolution, according to cardiovascular system parameters, where many of those are patient-specific. Moreover, these system models will be essential to design future communication links to realize pervasive networks of nanoscale wearable and implantable devices, i.e., the IoBNT [3]. In the following, we detail the specific functional blocks.

1) Information Encoding: The source information $X(t)$ is encoded into a proportional amount of information (or drug in PDDS context) molecules $N_D(t)$ present in the solution to be injected in the cardiovascular system, similar to (24).

2) Molecule Emission: The information molecules are emitted in the blood vessel at a predefined location of injection $\mathbf{p}_{Tx}$ (point-wise transmitter) by following a sequence of impulses emitted at a specific time interval T_s. According to [11], this models the behavior of a computer-controlled pump infusion syringe and, in general, expresses a molecule emission according to pulses (where $\delta(\cdot)$ might have a different shape than the Dirac's), e.g., emitted by engineered cells [13] in an IoBNT scenario. This is expressed as

$$\mathbf{p}_n(t_n) = \mathbf{p}_{Tx}, \quad n \in \left[0, \int_0^{t_n}\sum_{q=0}^{Q-1} N_D(t)\delta(t-qT_s)dt\right] \tag{70}$$

where Q is the total number of injection impulses.

3) Molecule Propagation: The emitted molecules propagate through the cardiovascular system according to Brownian motion with a drift velocity $\mathbf{v}(t,\mathbf{p})$ (4), which is a function of the time t and the location $\mathbf{p}$. The time dependence is a function of the heart pumping action while each molecule propagates, while the location dependence is a function of the location of the molecule at each time instant.

4) Molecule Reception: The emitted molecules propagate until reaching the location in the cardiovascular system where the receiver is located (in the PDDSs case, a blood vessel is in contact with the targeted tissue to be healed). The received signal corresponds to the particles present within a volume V_R surrounding the receiver, with a similar expression as in (26).

5) Information Decoding: The received molecules are recognized and absorbed by the receiver (diseased tissue in PDDSs, where the information they carry corresponds to the final healing action at the tissue itself). This is modeled as a quantity proportional to the number of received

molecules according to the molecule reception rate $p_D(t)$ as function of the time t, expressed as follows:

$$Y(t) = p_D(t) N_{\mathbf{R}}(t) \tag{71}$$

where $p_D(t)$ is expressed as [11]

$$p_D(t) = \pi r_o^2 m_R m_L e^{-\frac{\chi a \beta_w(t)}{k_B T_p r_0 m_R}\left(\left(\frac{a}{\gamma}+\psi\right)F_s + \frac{a^2}{r_0}R_s\right)} \tag{72}$$

where r_0 is the radius of the section of an information molecule, m_R is the density of chemical receptors at the surface of the receiver, m_L is the density of ligand/biomarkers at the surface of the molecules that can bind the receptors, k_B is Boltzmann's constant, T_p is the blood absolute temperature, F_s is the blood molecule drag force, R_s is the rotational moment of force on the molecule due to the blood flow, and $\beta_w(t)$ is the blood vessel wall sheer stress as function of the time t. Values or expressions of these parameters are detailed in [11].

6) Capacity: Given the generally accepted assumption that the blood flow in the vessels is laminar [12], the inhomogeneous advection–diffusion equation of this MC system is simplified into the Navier–Stokes equation. To determine if the flow is laminar, a metric known as the Reynolds number Re is used, where a laminar flow is characterized by $Re < 2300$. For blood flow in vessels, $Re \leq 2000$. The advection–diffusion equation in this scenario relates the information molecule distribution $\rho(\mathbf{p}, t)$ in every location of the cardiovascular system to the blood velocity $u_l(r, t)$ as a function of the radial coordinate r and the time t in the artery l of the cardiovascular system, expressed as follows [12]:

$$\frac{\partial \rho(\mathbf{p}, t)}{\partial t} = -\nabla.\left[-D\nabla\rho(\mathbf{p}, t) + u_l(r, t)\rho(\mathbf{p}, t)\right] + N_D(t)\delta(|\mathbf{p} - \mathbf{p}_{Tx}|). \tag{73}$$

The solution to (73) is found by applying the harmonic transfer matrix (HTM) theory [36] and transmission line theory [35] to express the transfer function of each artery and bifurcation in the cardiovascular system, as explained in [12]. Under the aforementioned assumption of laminar blood flow, as well as the assumptions that the blood velocity is homogeneous along the longitude of an artery, and that it only depends on the time variable t and the radial coordinate r in the artery, this corresponds to solving the Navier–Stokes equation [34], which relates the blood velocity vector $u_l(r, t)$ to the blood pressure $p(t)$ as functions of the time t. This is expressed as follows [12]:

$$\rho_B\left(\frac{\partial u_l(r, t)}{\partial t} + u_l(r, t)\cdot\nabla u_l(r, t)\right) = -\nabla p(t) + \mu\nabla^2 u_l(r, t) + f \tag{74}$$

where ρ_B is the blood density, which we assume homogeneous, μ is the blood viscosity, and f represents the contribution of blood vessel wall properties [37].

As a consequence of the aforementioned molecule reception and information decoding functional blocks, the probability distribution in the number of received molecules $N_{\mathbf{R}}$ is a Poisson counting process as in (29), where in this case, V_R is the volume surrounding the target tissue, as mentioned above.

The capacity C_{CV} of this MC system is computed in [11] by stemming from the aforementioned models. The final expression is as follows:

$$C_{\text{CV}} = T_S \sum_{r=1}^{R} \psi_m \left(\sum_{q=1}^{Q} \alpha_{q,r} A_q p_r\right) \tag{75}$$

where $\alpha_{q,r}$ summarizes the probability to successfully receive and decode an information molecule emitted at the qth interval, defined above, and received at the rth interval. A_n is the maximum nontoxic number of information molecules at the time qT_s, p_D is a coefficient depending on the aforementioned drug reception rate $p_D(t)$ that takes into account a full reception interval, R is the duration of the reception, divided into time intervals of duration T_s, Q is the aforementioned total number of injection pulses, and ψ_m takes into account noise sources at the injection, as described in [11].

C. Microfluidic Systems

Microfluidics is a technology that enables analysis and characterization of fluid dynamics at submillimeter-scale. Through the use of microchannels that allow a mixture of fluid to flow, the technology can allow integration of both chemical assay as well as molecular biology operations [80]. Examples of these operations include the ability to detect as well as separate out specific types of molecules on a Lab-on-Chip. MC systems have also been proposed for microfluidic systems [74], [76], [79]. Networks of microfluidic channels integrated with MC have been proposed to allow multiple steps of automated chemical analysis [74]. In [78], microfluidic-based MC was proposed for Network-on-chip communication, building on integrated microchannels that were cooling the computer processors.

Since the microfluidic system is considered as a simple version of a cardiovascular system, and it is known to be utilized for mixing different molecule types, the microfluidic structure considered has multiple transmitters and a single receiver, as illustrated in Fig. 10 [74]. The transmitters release molecules, which will diffuse through the microchannel, where the molecules will propagate under the influence of a flow with a constant drift velocity $\mathbf{v} = v_x$ according to (4) (we only consider a unidirectional flow along the x-axis). Therefore, multiple transmitters that do not have a centralized controller, such as a droplet register proposed in [78], can result in interference at

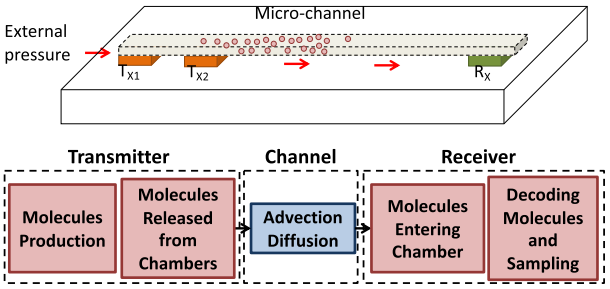

Fig. 10. ***Illustration of MC based on microfluidic systems.***

the receiver, impacting the capacity. This specific structure will be analyzed and discussed in this section, where the capacity will be derived based on the model proposed in [74].

1) Information Encoding: The encoding is achieved when a concentration of molecules is released to represent the source information $X(t)$. In this particular case, an OOK modulation scheme is used, where each of the transmitter chamber will produce $N_{\mathbf{T}}(t)$ molecules, which is based on (24).

2) Molecule Emission: The production rate of the molecules will depend on the frequency f_0 of $N_{\mathbf{T}}(t)$ production from a point source $\mathbf{p}_{T_x}$. This could be a population of cells that will coordinate to produce the molecules and diffuse into the environment [74]. For example, in [56], genetically engineered bacteria are placed in the transmitter chamber, and will collectively release molecules upon an external stimulus.

3) Molecule Propagation: The hydrodynamic properties of the fluid flow within the microchannel are governed by a Reynolds number $Re \ll 100$, which results in a velocity of the flow within the microchannel $\mathbf{v}(t, \mathbf{p})$ according to the Navier–Stokes equation.

4) Molecule Reception: The flow will create an advection drift that drives the molecules toward the receive chamber. The chamber will be a volume that receives the molecules, and it is assumed that the space will be large enough to capture the majority of the molecules (26).

5) Information Decoding: The molecules within the chamber will be sampled to determine the information that was transmitted. This will require synchronization between the transmitters as well as the receivers.

6) Capacity: There are similarities in the Fokker–Planck equation that was applied to the cardiovascular and the microfluidic system. According to (73), the information molecule distribution $\rho(\mathbf{p}, t)$ is dependent on the blood velocity $u_l(r, t)$. However, in the case of the microfluidic system, the location of the molecules is depending on the velocity along the x-axis $u_x(a, b, l)$, where a, b, and l are the microchannel height, width, and length, respectively. The Navier–Stokes equation can be solved toward an analytical solution for the flow velocity $u_x(a, b, l)$ of a rectangular-shaped channel, which is represented as

$$u_x(a, b, l) = \frac{a^2}{12\mu l}\mu l \left(1 - 0.63\frac{a}{b}\right) \Delta p \tag{76}$$

where μ is the viscosity of the fluid, and Δp is the pressure drop for the length of the channel.

According to [74], the received signal is represented as

$$y = \alpha x + n \tag{77}$$

where x is the number of transmitted encoded molecules [equal to $N_{\mathbf{T}}(t)$ in the general framework], α is the channel gain, and n is the channel noise. Since we are considering multiple transmitters, the gain α in (77) is defined as an end-to-end channel gain α_{ij} for interfering signals from j transmitters to receiver i and is expressed as

$$\alpha_{ij} = \alpha_{\text{ch}}^{ij} \alpha_{\text{tx/rx}}^2 \tag{78}$$

where the gain of the transmitter and receiver $\alpha_{\text{tx/rx}}$ is

$$\alpha_{\text{tx/rx}} = \exp\left(-\frac{4\pi^2 f_0^2}{u_{\text{tx/rx}}^2} D_0 \tau_{\text{tx/rx}}\right) \text{sinc}\left(\frac{a_{\text{tx/rx}}}{u_{\text{tx/rx}}} f_0\right) \tag{79}$$

where $a_{\text{tx/rx}}$ is the width of the transmitter and the receiver chamber, $u_{\text{tx/rx}}$ is the propagation velocity, $\tau_{\text{tx/rx}}$ is the propagation delay from the chamber to the microchannel, and f_0 is the rate of molecules release from the transmitter. The signal gain of the channel α_{ch} is represented as

$$\alpha_{\text{ch}} = \exp\left(-\frac{4\pi^2 f_0^2}{u_{\text{ch}}^2} D \tau_{\text{ch}}\right) \tag{80}$$

where τ_{ch} is the propagation delay along the microchannel, u_{ch} is the propagation velocity, and D is the Taylor dispersion adjusted diffusion coefficient for the rectangular microfluidic channels.

According to [74], at low frequencies of emitted molecules from the transmitter chamber, the spectral density of the received molecule signal is assumed to be flat. This means that the noise can be considered as additive white Gaussian noise (AWGN), and this is represented as

$$\sigma^2 = \left(2\alpha_{\text{tx/rx}}^4 \frac{D\tau_{\text{ch}}}{u_{\text{ch}}^2} + 4\frac{D_0 \tau_{\text{tx/rx}}}{u_{\text{tx/rx}}^2} \alpha_{\text{ch}}^2 \alpha_{\text{tx/rx}}^2\right) 4\pi^2 f_0^2 \phi^2. \tag{81}$$

The magnitude of the interference from the different transmitters will also need to be considered. The variance of the interference from transmitter j on the receiver i is represented as

$$\zeta_{ij}^2 = \left(\alpha_{\text{ch}}^{ij}\right)^2 \alpha_{\text{tx/rx}}^4 \phi_j^2. \tag{82}$$

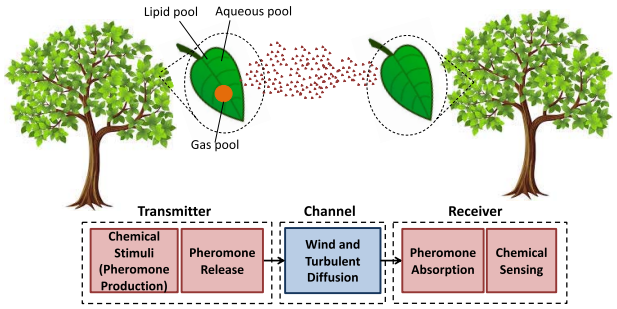

Fig. 11. *Illustration of MC based on pheromone communication.*

There is also an induced noise from the interfering transmitters within the microfluidic channel. The variance of the intefering transmitter j on receiver i is represented as

$$\xi_{ij}^2 = \left(1 - (\alpha_{\text{ch}}^{ij})^2\right)\alpha_{\text{tx/rx}}^4 \phi_j^2. \tag{83}$$

Based on the above-mentioned equations, the capacity for a microfluidic system with a single receiver i and multiple transmitters, where certain transmitter can act as interferers, is represented as follows:

$$C_i = \frac{1}{T_0}\log_2\left(1 + \frac{\alpha_{ii}^2\phi_i^2}{\sigma_i^2 + \sum_{j=2}^{N}\zeta_{ij}^2 + \xi_{ij}^2}\right) \tag{84}$$

where there are, in total, N transmitters, and ϕ_i^2 is the signal variance at the receiver i. This expression is for the case where there is one transmitter (Tx_1) and $N-1$ interfering transmitters.

D. Pheromone Communication

Since the original vision of MC is to exploit biological communication systems to enable nanomachines to communicate, the majority of the distances considered is between nano to centimeter scale. However, a form of MC was studied that enables information to propagate up to a few meters and beyond, i.e., through pheromones [57], which is illustrated in Fig. 11. Pheromones are used as chemical signaling by plants, insects, and animals. A good example for insects is in bee colonies, where pheromones are used by the queen to signal worker bees toward reproduction. Pheromone communication is part of the approaches brought out by evolution for maintaining the vegetation ecosystems. In this MC system, molecules are released into the atmosphere and propagate to the destination by means of turbulent diffusion, which is a form of Brownian motion with drift, where the latter is stochastic in nature.

1) Information Encoding: The emission of the pheromones is produced in the secretory cells of the plants, and they are usually stored before their emission, which is stimulated by excitation. The excitation process in many cases is based on an external stimulus (e.g., an attack that is sensed by the plants). The storage of the pheromone molecules is realized through both the aqueous pools (S_A) and lipid phase pools (S_l) inside each cell. These are intermediate storage points, before they diffuse to the intercellular air space on the plant leaves, where they are stored in gas pools. From the gas pools, they will diffuse through the leaf stomata into the air. The encoding of the information can be achieved through the stimulation of the secretory cells, and the consequent rate of the emitted pheromone molecules. Although the way pheromones are used to encode information in nature is still an open question for most cases, this paper abstracts information transmission through pheromones as an OOK system, where secretory cells are stimulated according to a digital bit stream.

2) Molecular Emission: The rate of release from the aqueous storage pools (S_A) is k_A, and from the lipid phase storage pools (S_l) is k_l. Based on this, the molecules will be stored in the gas phase (S_g), which is in the leaf intercellular air space. The rate of release of the pheromone flux from the gas phase storage is k_g. The models for each of these release processes, in the form of chemical kinetics expressions (3), are as follows:

$$\begin{aligned}
\frac{dS_a(t)}{dt} &= \eta s(t) - k_a S_a(t) \\
\frac{dS_l(t)}{dt} &= (1-\eta)s(t) - k_l S_l(t) \\
\frac{dS_g(t)}{dt} &= k_a S_a(t) + k_l S_l(t) - k_g S_g(t)
\end{aligned} \tag{85}$$

where η is the ratio of the synthesized pheromones between the aqueous and lipid phase. The emission rate of the volatile pheromones from the leaf is $q(t) = k_g S_g(t)$, where the $q(t)$ is the emitted signal by the leaves of the plants. Based on these models, in [57], the normalized gain for the attenuated pheromone signal that is diffused from the cells to the intercellular air space, and then to the air, is developed, including the delay of the transmission process. The release of pheromones is operated at the gas pools, as defined in (8), where S_T is now the volume of these pools, and $N_{\mathbf{T}}(t)$ corresponds to the pheromone emission rate $q(t)$.

3) Molecular Propagation: Once the pheromones are secreted from the plants, the propagation is assisted by air flows, and this results in the aforementioned turbulent diffusion. In [57], a 1-D flow of wind was considered to derive tractable mathematical expression for the distribution $\rho(\mathbf{p}, t)$ of propagating pheromones. The model considered the mass flux of pheromones due to both advection caused by wind, as well as atmospheric diffusion subject to turbulent eddy motion. A number of assumptions were considered in this model, and this includes: 1) wind velocity is consistent and aligns along the x-axis;

2) diffusion is isotropic and the eddy diffusivities K in $(x; y; z)$ depend only on the downwind distance ($K_x(x) = K_y(x) = K_z(x) =: K(x)$); 3) wind velocity is significantly large so that the diffusion along the x-axis is negligible; 4) there is only one source of the pheromone emission; and 5) the mass of the pheromones remains finite. Based on these conditions, the distribution $\rho(\mathbf{p}, t)$ defined in [57] is expressed as follows:

$$\rho(\mathbf{p},t) = q(t) * \frac{1}{8(\pi r)^{3/2}} e^{(-(x-ut)^2-y^2)/4r} \times [e^{-(z-H)^2/4r} + e^{-(z+H)^2/4r}] \quad (86)$$

where $q(t)$ is the pheromone distribution a time t, $*$ is the convolution operation, $r = (1/u)\int_0^x K\xi dx$, and H is the height of the emitting leaf from the ground.

$\rho(\mathbf{p}, t)$ can be further adopted to consider anisotropic eddy diffusivities for y- and z-directions, $K_y(x) \neq K_z(x)$, and this is represented as

$$\rho(\mathbf{p},t) = q(t) * \frac{1}{8(\pi r)^{3/2}} e^{\frac{(-(x-ut)^2-y^2)}{4\sqrt{r_y r_z}}} e^{\frac{(-y^2)}{4r_y}} \times [e^{-(z-H)^2/4r_z} + e^{-(z+H)^2/4r_z}]. \quad (87)$$

4) Molecular Reception: Once the pheromones arrive at the destination plant, they will be absorbed by the leaves of plants that are from the same species as the transmitting plant. As a first step, there is a gas exchange through miniature openings in the leaves known as the stomata. The net flux of pheromones for the gas exchange is represented as

$$\Phi = Ag[\rho(\mathbf{p},t)|_{\mathbf{p}\in S_R} - C_L(t)/K_{LA}] \quad (88)$$

where A is the area of the leaf surface S_R, g is the conductance, K_{LA} is the partition coefficient and represents the concentration ratio between air and leaves at thermodynamic equilibrium, $\rho(\mathbf{p}, t)$ is the concentration of the pheromones in the air that arrives at the leaves, while $C_L(t)$ is the concentration of pheromones in the leaves [57]. By considering the mass in the pheromones on the aerial side and the volume V_L of the leaves, the change in concentration of the pheromones inside the leaves can be represented as

$$\frac{dc_L(t)}{dt} = -\left(\frac{A_g}{K_{LA}V_L}\right) C_L(t) + \left(\frac{A_g}{V_L}\right) \rho(\mathbf{p},t)|_{\mathbf{p}\in S_R}. \quad (89)$$

5) Information Decoding: Once the pheromones enter the stomata of the leaves, they will diffuse through Brownian motion into different layers that include the spongy and palisade layers of the leaves [57]. At this point, the diffused pheromones will be transformed into a number of different chemicals, where they may result in cell physiological responses. The decoding process can therefore be abstracted as the interpretation of the changes in the concentrations of the pheromones in relation to these physiological responses.

6) Capacity: To date, there has been no capacity model developed for pheromone communications. The work in [57] defined the channel model by expressing the channel gain as well as the delay. This analysis was developed for the gain and delay of the molecular emission (Γ_T, $\tau_T(f)$), propagation (Γ_P, $\tau_P(f)$), as well as the absorption into the leaves at the receiver (Γ_R, $\tau_R(f)$). Based on these, the normalized gain of the system is determined ($\Gamma(f) = \Gamma_T(f) \cdot \Gamma_P(f) \cdot \Gamma_R$), as well as the end-to-end delay ($\tau(f) = \tau_T(f) + \tau_P(f) + \tau_R(f)$). The limitations of this model are the consideration of only a 1-d flow of drift. Besides the requirements for closed-form capacity expressions, there are numerous research issues that need to be considered. This includes the impact on the types of pheromones that are generated from different types of leaves and plants. Numerous research projects have focused on understanding plant communication as they face varying environmental impact (e.g., effects of drought and pathogen attacks). However, an open research for the future is the understanding of how these environmental changes impact the capacity of pheromone communication, which could lead to new approaches for monitoring the ecological changes.

V. MOLECULAR COMMUNICATION VIA ACTIVE TRANSPORT

Although the MC systems that have been presented so far have focused on random walk, and drifted random walk under the influence of an independent velocity, in MC systems based on active transport, the molecules emitted by the transmitter propagate by means of the Brownian-motion-independent force $\mathbf{F}_n(t)$ and the Brownian motion $\mathbf{f}(t)$. This is modeled by the Langevin equation in (4) where the drift velocity $\mathbf{v}_n(t)$ of the fluid is set to zero. In the following, we revise the Brownian motion capacity expressed in Section III-A through the definition of a basic abstraction of an MC system via active transport. Subsequently, we detail the functional block models of MC systems based on active transport that have been studied, namely, MC based on bacteria chemotaxis and molecular motors.

A. Ornstein–Uhlenbeck Channel Capacity

The basic abstraction of an MC system via active transport is shown in Fig. 12. In the following, we describe the differences in the channel model with respect to the Brownian motion channel detailed in Section III-A.

1) Molecule Propagation: Molecules propagate by virtue of the Brownian motion and an external force $\mathbf{F}_n(t) = \theta\,|\mathbf{p} - \mathbf{p}_{Rx}|$ that is proportional with respect to the distance of the particle itself to a location in space, here considered as the location of the receiver $\mathbf{p}_{Rx}$, where θ is a constant

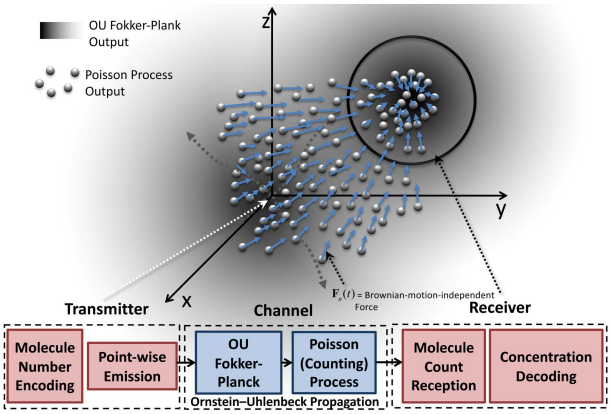

Fig. 12. ***Basic abstraction of an MC system based on active transport.***

parameter that controls the strength of the system to react to perturbations. This propagation process is known as the Ornstein–Uhlenbeck (OU) process [70]. As in Section III-A, we make the assumption to have a 3-D space with infinite extent in every dimension.

2) Capacity: As a consequence of the aforementioned molecule propagation, the Fokker–Planck equation (17) for this MC system corresponds to the inhomogeneous OU Fokker–Planck equation [7], expressed as follows:

$$\frac{\partial \rho(\mathbf{p},t)}{\partial t} = D\nabla^2 \rho(\mathbf{p},t) - \theta \nabla \left|\mathbf{p}-\mathbf{p}_{Rx}\right| \rho(\mathbf{p},t) + N_{\mathbf{T}}(t)\delta(|\mathbf{p}-\mathbf{p}_{Tx}|). \quad (90)$$

Similarly to what was stated in Section IV-A, the Poisson point process (19) that models the particle location displacement $\mathbf{p}_n(t)$ becomes a Poisson counting process, as expressed in (29).

The entropy $H(\rho)$ of the particle distribution ρ can be analytically expressed as in (65), where this time $h_{\text{Adv}}(\mathbf{p}_{Tx},\mathbf{p}_{Rx},t)$ is substituted with $h_{\text{OU}}(\mathbf{p}_{Tx},\mathbf{p}_{Rx},t)$, which is equal to the impulse response of (90), expressed as follows [7]:

$$h_{\text{OU}}(\mathbf{p}_{Tx},\mathbf{p}_{Rx},t) = \sqrt{\frac{\theta}{2\pi D(1-e^{-2\theta t})}} e^{-\frac{\theta}{2D}\left[\frac{\left(\left(|\mathbf{p}_{Tx}-\mathbf{p}_{Rx}|\right)e^{-\theta t}\right)^2}{1-e^{-2\theta t}}\right]}. \quad (91)$$

As for Fick's second law in Section III-A, and the advection–diffusion in Section IV-A, also the OU Fokker–Planck equation in (90) and (91) corresponds to a linear and time-invariant filter applied to the modulated number $N_{\mathbf{T}}(t)$ of emitted molecules. Consequently, we can apply the formula in (32) where the term $H_{\text{Diff}}(f)$ is substituted with $H_{\text{OU}}(f)$, which is the Fourier transform of the impulse response in (91), which does not have an analytical solution, but has to be computed numerically as in (67). With a similar derivation as in (68) and (36), and since $H_{\text{OU}}(f)$ does not depend on the probability distribution of the modulated number of molecules $N_{\mathbf{T}}(t)$, the capacity C_{OU} of the OU channel is then obtained similar to Section IV-A, resulting into the same expression as in (38) with $H_{\text{OU}}(f)$ in place of $H_{\text{Adv}}(f)$.

B. Bacterial Chemotaxis

The bacterial chemotaxis differs from the previous MC systems, given that it utilizes an organism to carry the information to deliver to a target [65]–[67]. The bacterial chemotaxis enables a communication system to be constructed for a medium-range nanonetwork. Fig. 13 illustrates the communication process for a bacterial chemotaxis. The information is encoded into a DNA plasmid, which is inserted into a bacterium cell (bacterium transformation) through the process of conjugation. The bacterium will then move toward the receiver by harnessing chemical energy to deliver the DNA plasmid. The bacterium can direct its motion according to chemical trails created by other diffusing molecules, i.e., chemoattractants, emitted from the receiver location. Examples of chemotaxis from nature are bacteria in search of food, or environmentally favorable locations. The distribution of chemoattractant when continuously emitted by the receiver can be modeled as follows:

$$U(r,t) = \frac{Q}{2D\pi r}\,\text{erfc}\left(\frac{r}{\sqrt{4Dt}}\right) \quad (92)$$

where $\text{erfc}(x) = (2/\sqrt{\pi})\int_x^\infty e^{-t^2}dt$, r is the distance from the source of chemoattractant emission, t is the time, and D is the chemoattractant diffusion coefficient. The assumptions taken for the chemoattractant gradient are an even spatial homogeneity as the concentration diffuses into the environment, and no obstacles present in the space.

1) Information Encoding: The information to be transmitted is encoded into a DNA plasmid, which lies inside the transmitter. Encoding digital data into DNA is a

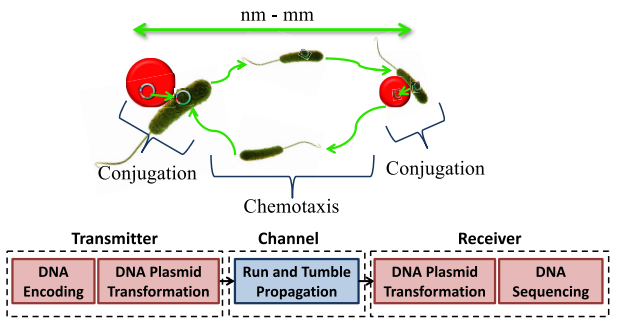

Fig. 13. ***Illustration of an MC system based on bacterial chemotaxis.***

well-studied area that gained particular attention in recent years [69]. The simplest form of encoding is using two bit/nucelotide. Based on this, a message that can be encoded per plasmid is approximately 600 Kbits (which is 300K base pairs for two bit/nucleotide encoding). This corresponds to encoding an intensive property as follows (6):

$$nu_k = A_1(X(t_k)) \quad k = 1, 2 \ldots, K \tag{93}$$

where K defines the length of the encoded DNA plasmid, nu_k defines the kth plasmid encoded with the source information value $X(t_k)$ at time t_k, and A_1 abstracts encoding technique that is used to convert the source information into DNA nucleotide values.

2) Molecular Emission: The motile bacterium can pick up the encoded DNA plasmid through the process of transformation [66], which enables the DNA plasmid to be adsorbed into the membrane of the cell. Another technique is through conjugation [67], where bacteria form physical connections to share copies of the DNA plasmids. As a result, the plasmid molecule is emitted at the transmitted location $\mathbf{p}_{Tx}$ at the transmission time t_0, expressed as

$$\mathbf{p}(t_0) = \mathbf{p}_{Tx} \tag{94}$$

where $\mathbf{p}(t_0)$ is the location of the plasmid molecule at time of emission t_0. The assumptions taken are similar to those underlying (17), where the emitted plasmid molecules are considered spherical, at low concentration, and subject to free diffusion.

3) Molecular Propagation: The motility process of the bacterium loaded with the emitted plasmid is based on a repetitive series of Run and Tumble phases [65]. During the running period, the bacterium swims at a constant speed of 20 μm for a random period t_{run}. During this period, the bacterium will change its angle θ based on a Gaussian probability density function where $E[\theta^2] = 2D_{\text{rot}}t$, where t is the swimming time within t_{run} and D_{rot} is the rotational diffusion coefficient and represented as

$$D_{\text{rot}} = \frac{k_B T}{8\pi\eta a^3} \tag{95}$$

where η is the fluid viscosity, a is the bacterium's radius, T is the temperature. After t_{run}, the bacterium switches to a tumbling phase. The distribution of t_{run} is expressed as follows:

$$p(t_{\text{run}}, 1/\alpha(u)) = \frac{1}{\alpha(u)} e^{\frac{-t_{\text{run}}}{\alpha(u)}} \tag{96}$$

where $\alpha(u)$, as function of the chemoattractant distribution $u(t) = U(r,t)|_{r=\mathbf{p}(t)}$, where $\mathbf{p}(t)$ is the location of the bacterium/DNA plasmid at time t, can be formalized as [65]

$$\alpha(U) = \begin{cases} \alpha_0 - g\displaystyle\int_0^\infty u(t)h(t-\tau)d\tau, & u(t) * h(t) > 0, \\ \alpha_0, & u(t) * h(t) \leq 0 \end{cases} \tag{97}$$

where α_0 is the base run duration of 1 s, and g is the bacterium sensitivity, and $*$ is the convolution operator. During the tumbling period, the bacterium will change its angle θ as follows [65]:

$$\theta_{n+1} = \theta_n + \gamma \tag{98}$$

where θ_{n+1} is the angle at the nth tumbling phase, and γ is a random variable with the following distribution:

$$f(\gamma) = \begin{cases} \frac{1}{4}\cos\left(\frac{\gamma}{2}\right), & |\gamma| \leq \pi \\ 0, & |\gamma| > \pi. \end{cases} \tag{99}$$

The tumble phase duration t_{tumble} is based on the following probability:

$$p(t_{\text{tumble}}, \mu) = \frac{1}{\mu} e^{\frac{-t_{\text{tumble}}}{\mu}} \tag{100}$$

where μ =1 s. This, effectively, results in the bacterium switching the phases based on a two-state Markov chain, and in the propagation of the encoded DNA plasmid.

4) Molecular Reception: Once the bacterium approaches the receiver, it will offload the DNA plasmid. In a similar approach taken by the information encoding, this can be through conjugation, where the physical connection will transfer copies of the DNA plasmid to the receiver. This will happen when the bacterium/DNA plasmid location will be equal to the receiver location, namely, $\mathbf{p}(t) = \mathbf{p}_{Rx}$. The probability of successful conjugation will highly depend on the species of the bacteria as well as the types of plasmids used.

5) Information Decoding: The DNA plasmid that is retrieved from the bacterium will be sequenced in order to obtain the encoded information, expressed as

$$[\widehat{X}(t_1), \widehat{X}(t_2), \widehat{X}(t_K)] = A_1^{-1}([nu_1, nu_2, \ldots, nu_K]). \tag{101}$$

6) Capacity: The capacity of an MC system based on chemotaxis was estimated in [65]. This capacity calculation considers the stochastic nature of the aforementioned emission process, as well as mutation effects that can distort the information encoded in the DNA plasmid. As an extension, the estimation of a multihop nanonetwork capacity was also proposed in [65]. However, there is

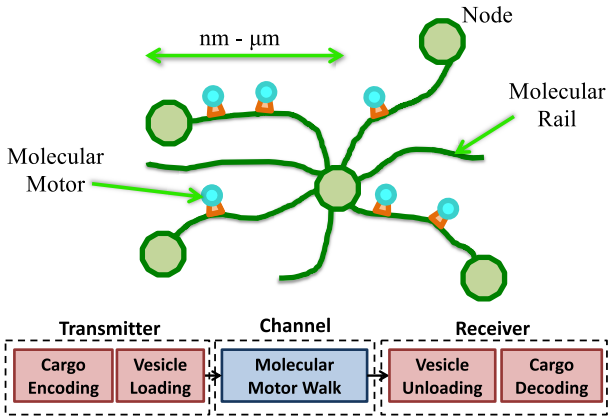

Fig. 14. *Scheme of an MC sytem based on molecular motors.*

still a requirement for a closed-form expression for the capacity of bacterial chemotaxis, and in particular for a population of bacteria. A closed-form expression can also result in new models that can be used to develop novel applications, such as accurate novel gene therapies. Impact of bacterial social structures on the end-to-end capacity is also required. To date, only the attenuation has been considered for a simple bacterial chemotaxis system, which only considers competition and cheating for a small population [68]. A major contribution is how the social dynamics between the different species can impact DNA transfer between the bacteria, and how this, in turn, impact the stability of the microbiome, which is an environment of multiple bacterial species coexisting together.

C. Molecular Motors

A good example of MC based on active transport occurs within a cell [72], [77]. Cells contain rails known as filaments or microtubules that connect the membrane and the nucleus, and they are flexible structures. The microtubules contain a mobile unit that walks on the rail and carries cargoes between the cell membrane and the nucleus. These mobile units are known as molecular motors and harness chemical energy from adenosine triphosphate (ATP) hydrolysis to produce mechanical motion [71]. Fig. 14 illustrates an MC system that utilizes molecular motors to realize multiple communication links, where encoded information are inserted into vesicles that are placed on molecular motors, which walk along the molecular rail that connect different nodes, until the delivery of the cargo to the receiver. This energy conversion enables the molecular motor to walk as well as rotate on the microtubule rails. The size of each molecular motor ranges from few nanometers to tens of nanometers and carry cargo using a vesicle that encapsulates molecules. Specific examples are myosin molecular motors, which walk on filaments tracks or the pull these filaments to enable muscle motion, while kinesinand dynein move along microtubules. Molecular motors are able to mobilize cargoes of varying sizes, and examples include entire cell organelles (e.g., mitochondria) and vesicles (e.g., lysosomes and endosomes) [71].

1) Information Encoding: The encoding process can be conducted on a DNA or messenger ribonucleic acid (mRNA), and this is inserted into a 200-nm vesicle. The encoding process can be conducted using (93). Given that the DNA or mRNA can hold a large quantity of information, this means that the majority of transmitted information can be carried by a single molecular motor.

2) Molecular Emission: Once a vesicle is loaded onto a molecular motor, it will detach from the membrane of the cell and align itself onto the microtubule rail to start is motility. The rate of emission will depend on the vesicle loading process onto the molecular motor. The molecule location will be abstracted with the transmitted location, similar to (94).

3) Molecular Propagation: The molecular motor converts energy to mechanical movement as it walks along the microtubule rails [71]. The speed of the molecular motor, which is estimated to amount up to $\nu_{\max} = 0.1\ \mu$s, can be expressed as a function of the chemical energy as follows [72]:

$$\nu = \frac{\nu_{\max} c_{\text{ATP}}}{c_{\text{ATP}} + K_{\text{ATP}}} \tag{102}$$

where c_{ATP} and K_{ATP} are a form of ATP energy. There is a certain amount of stochastic randomness as the molecular motors walk along the rails, which is a repetitive forward and backward motion. In this paper, we only consider a single-link model of the molecular motor mobility. In [72], a 1-D Fokker–Planck equation was used to evaluate the probability density function $\rho(x,t)$, which models the random location of the molecular motor on the rail (along the coordinate x) as function of the time t. The Fokker–Planck equation is represented as

$$\frac{\partial \rho(x,t)}{\partial t} = -V\frac{\partial \rho(x,t)}{\partial x} + D\frac{\partial^2 \rho(x,t)}{\partial x^2} - \Lambda\rho(x,t) \tag{103}$$

where D is the diffusion coefficient, V is the drift term, and Λ is the reaction term. The diffusion coefficient D is expressed as

$$D = \frac{2\nu^2}{\gamma^3 \beta_+^2 \beta_-^2 \alpha^2}(\beta_-^2 - 4\alpha^2 + 2\alpha\beta_- + \alpha\beta_+ + \alpha\beta_-) \tag{104}$$

where $\gamma = 1/\beta_+ + 1/\beta_- + 1/\alpha$, β is the detachment rate (when the molecular motor is in the backward motion, the rate is β_-, and in the forward motion, it is β_+), κ is the rate of detachment from the rail, α is the rate of going either forward or backward in the case of a reattachment. The diffusion component D plays a role when the molecular motor detaches from the rails. Given that their weight is extremely low, their motion can be affected from the

turbulence of the fluids within the environment. Once they detach off the rails, they can randomly land on a separate rail and continue walking. The detachment process is proportional to the distance traveled from the cell membrane, and this is based on an exponential distribution with a mean of 100 μm. The aforementioned drift term V represents the walking motion of the molecular motors and is expressed as

$$V = \frac{\nu}{\gamma}\left(\frac{1}{\beta_+} - \frac{1}{\beta_-}\right) \tag{105}$$

and the reaction term Λ is expressed as

$$\Lambda = \frac{\kappa}{\gamma\alpha} \tag{106}$$

4) Molecular Reception: Once the molecular motor arrives at the receiver, it will be detached from the rail and will unload the vesicles. This will happen when the vesicle location will be equal to the receiver location, namely, $\mathbf{p}(t) = \mathbf{p}_{Rx}$. One approach for addressing at the receiver is to use the concept of DNA hybridization proposed in [82].

5) Information Decoding: The decoding process will be sequencing of the DNA or mRNA to retrieve the encoded information, as in (101).

6) Capacity: In [72] an impulse response was validated numerically to determine the position of the molecular motor along a rail, which was compared to simulations. The simulations were also conducted on a bipartite tree network, in order to evaluate the presence of the molecular motors in links with a number of separating nodes. This simulation considered the network topology of the microtubule rails within the neurons. A capacity model was proposed in [77], for both unicast as well as broadcast molecular motors communication. However, this was not a closed-form expression, but rather empirical measurements that were used to define the mutual information. Therefore, a step forward would be the development of a closed-form expression. The closed-form model should consider how the vesicle cargo can impact the communication performance, and how this can dynamically change a cell's functionality.

VI. CONCLUSION

In this paper, we have proposed a general framework to analyze the information-theoretic performance of MC systems. In particular, we have defined a theoretic view of diverse implementations of MC based on their underlying physical and chemical processes. In this direction, we have classified known MC systems into three different categories on the basis of the way molecules are propagated between the transmitter and the receiver. For each category, we have provided a general methodology to compute or estimate information capacity, as well as a discussion of the impact of the functional block of each specific system on the overall performance.

The multidisciplinary nature of MC will require close collaborations with fields in natural science, particularly molecular biology, medicine, and chemistry. This collaboration will foster this field and, at the same time, provide a testing ground for validating as well as refining the models that have been proposed in more than a decade of MC-focused research. The future will also require new medical and biotechnology applications that can utilize MC as a supporting tool, complementing existing practices, such as in [10]–[12]. The statistical-mechanics-based framework that has been proposed in this paper provides a common ground that not only allows existing researchers in this field to recap the direction that has been taken in the last decade but also provides future researchers with a well-defined methodology to evaluate the performance of MC systems. This will enable novel investigation directions and research results that build on the developed capacity models. We believe this contribution will be foundational for this discipline, and an important milestone for the engineering of future MC systems. ■

REFERENCES

[1] I. F. Akyildiz, F. Brunetti, and C. Blázquez, "Nanonetworks: A new communication paradigm," *Comput. Netw.*, vol. 52, no. 12, pp. 2260–2279, Aug. 2008.

[2] I. F. Akyildiz, J. M. Jornet, and M. Pierobon, "Nanonetworks: A new frontier in communications," *Commun. ACM*, vol. 54, no. 11, pp. 84–89, Nov. 2011.

[3] I. F. Akyildiz, M. Pierobon, S. Balasubramaniam, and Y. Koucheryavy, "The Internet of bio-nano things," *IEEE Commun. Mag.*, vol. 53, no. 3, pp. 32–40, Mar. 2015.

[4] T. Nakano, M. J. Moore, F. Wei, A. V. Vasilakos, and J. Shuai, "Molecular communication and networking: Opportunities and challenges," *IEEE Trans. Nanobiosci.*, vol. 11, no. 2, pp. 135–148, Jun. 2012.

[5] D. L. Nelson and M. M. Cox, *Lehninger Principles of Biochemistry*. San Francisco, CA, USA: Freeman, 2005, ch. 12.2, pp. 425–429.

[6] T. M. Cover and J. A. Thomas, *Elements of Information Theory*, 2nd ed. Hoboken, NJ, USA: Wiley, 2006.

[7] H. Risken and T. Frank, *The Fokker-Planck Equation: Methods of Solution and Applications*. Springer, 1996.

[8] E. L. Cussler, *Diffusion: Mass Transfer in Fluid Systems*, 2nd ed. Cambridge, U.K.: Cambridge Univ. Press, 1997.

[9] M. P. Langevin, "Paul Langevin's 1908 paper 'On the theory of Brownian motion,'" *Amer. J. Phys.*, vol. 65, no. 11, pp. 1079–1081, Nov. 1997.

[10] Y. Chahibi, M. Pierobon, and I. F. Akyildiz, "Pharmacokinetic modeling and biodistribution estimation through the molecular communication paradigm," *IEEE Trans. Biomed. Eng.*, vol. 62, no. 10, pp. 2410–2420, Oct. 2015.

[11] Y. Chahibi and I. F. Akyildiz, "Molecular communication noise and capacity analysis for particulate drug delivery systems," *IEEE Trans. Commun.*, vol. 62, no. 11, pp. 3891–3903, Nov. 2014.

[12] Y. Chahibi, M. Pierobon, S. O. Song, and I. F. Akyildiz, "A molecular communication system model for particulate drug delivery systems," *IEEE Trans. Biomed. Eng.*, vol. 60, no. 12, pp. 3468–3483, Dec. 2013.

[13] C.-H. Chuang and C.-L. Lin, "Synthesizing genetic sequential logic circuit with clock pulse generator," *BMC Syst. Biol.*, vol. 8, no. 1, p. 63, May 2014.

[14] C. E. Shannon, "A mathematical theory of communication," *Bell Syst. Tech. J.*, vol. 27, no. 3, pp. 379–423, Jul./Oct. 1948.

[15] M. Pierobon and I. F. Akyildiz, "Capacity of a diffusion-based molecular communication system with channel memory and molecular noise," *IEEE Trans. Inf. Theory*, vol. 59, no. 2, pp. 942–954, Feb. 2013.

[16] M. Pierobon and I. F. Akyildiz, "Noise analysis in ligand-binding reception for molecular communication in nanonetworks," *IEEE Trans. Signal Process.*, vol. 59, no. 9, pp. 4168–4182, Sep. 2011.

[17] M. Pierobon and I. F. Akyildiz, "A physical end-to-end model for molecular communication in nanonetworks," *IEEE J. Sel. Areas Commun.*, vol. 28, no. 4, pp. 602–611, May 2010.

[18] V. Jamali, A. Ahmadzadeh, C. Jardin, C. Sticht, and R. Schober, "Channel estimation for diffusive

molecular communications," *IEEE Trans. Commun.*, vol. 64, no. 10, pp. 4238–4252, Oct. 2016.
[19] A. Marcone, M. Pierobon, and M. Magarini, "Parity-check coding based on genetic circuits for engineered molecular communication between biological cells," *IEEE Trans. Commun.*, vol. 66, no. 12, pp. 6221–6236, Dec. 2018.
[20] T. Nakano, Y. Okaie, and J. Q. Liu, "Channel model and capacity analysis of molecular communication with Brownian motion," *IEEE Commun. Lett.*, vol. 16, no. 6, pp. 797–800, Jun. 2012.
[21] Y. Murin, N. Farsad, M. Chowdhury, and A. Goldsmith, "Exploiting diversity in one-shot molecular timing channels via order statistics," *IEEE Trans. Mol. Biol. Multi-Scale Commun.*, vol. 4, no. 1, pp. 14–26, Mar. 2018.
[22] B. Krishnaswamy *et al.*, "Time-elapse communication: Bacterial communication on a microfluidic chip," *IEEE Trans. Commun.*, vol. 61, no. 12, pp. 5139–5151, Dec. 2013.
[23] N. Farsad, C. Rose, M. Médard and A. Goldsmith, "Capacity of molecular channels with imperfect particle-intensity modulation and detection," in *Proc. IEEE Int. Symp. Inf. Theory (ISIT)*, Aachen, Germany, Jun. 2017, pp. 2468–2472.
[24] C. Rose and I. S. Mian, "Inscribed matter communication: Part I," *IEEE Trans. Mol. Biol. Multi-Scale Commun.*, vol. 2, no. 2, pp. 209–227, Dec. 2016.
[25] C. Rose and I. S. Mian, "Inscribed matter communication: Part II," *IEEE Trans. Mol. Biol. Multi-Scale Commun.*, vol. 2, no. 2, pp. 228–239, Dec. 2016.
[26] G. Aminian, H. Arjmandi, A. Gohari, M. Nasiri-Kenari, and U. Mitra, "Capacity of diffusion-based molecular communication networks over LTI-Poisson channels," *IEEE Trans. Mol. Biol. Multi-Scale Commun.*, vol. 1, no. 2, pp. 188–201, Jun. 2015.
[27] L. Felicetti, M. Femminella, G. Reali, T. Nakano, and A. V. Vasilakos, "TCP-like molecular communications," *IEEE J. Sel. Areas Commun.*, vol. 32, no. 12, pp. 2354–2367, Dec. 2014.
[28] L. Canzian, K. Zhao, G. C. L. Wong, and M. van der Schaar, "A dynamic network formation model for understanding bacterial self-organization into micro-colonies," *IEEE Trans. Mol. Biol. Multi-Scale Commun.*, vol. 1, no. 1, pp. 76–89, Mar. 2015.
[29] P.-J. Shih, C.-H. Lee, P.-C. Yeh, and K.-C. Chen, "Channel codes for reliability enhancement in molecular communication," *IEEE J. Sel. Areas Commun.*, vol. 31, no. 12, pp. 857–867, Dec. 2013.
[30] Y. Lu, M. D. Higgins, and M. S. Leeson, "Comparison of channel coding schemes for molecular communications systems," *IEEE Trans. Commun.*, vol. 63, no. 11, pp. 3991–4001, Nov. 2015.
[31] R. Mosayebi, H. Arjmandi, A. Gohari, M. Nasiri-Kenari, and U. Mitra, "Receivers for diffusion-based molecular communication: Exploiting memory and sampling rate," *IEEE J. Sel. Areas Commun.*, vol. 32, no. 12, pp. 2368–2380, Dec. 2014.
[32] S. M. Mustam, S. K. Syed-Yusof, and S. Zubair, "Capacity and delay spread in multilayer diffusion-based molecular communication (DBMC) channel," *IEEE Trans. Nanobiosci.*, vol. 15, no. 7, pp. 599–612, Oct. 2016.
[33] G. Aminian, M. Farahnak-Ghazani, M. Mirmohseni, M. Nasiri-Kenari, and F. Fekri, "On the capacity of point-to-point and multiple-access molecular communications with ligand-receptors," *IEEE Trans. Mol. Biol. Multi-Scale Commun.*, vol. 1, no. 4, pp. 331–346, Dec. 2015.
[34] M. Potter and D. Wiggert, *Fluid Mechanics* (Schaum's Outlines Series). New York, NY, USA: McGraw-Hill, 2008.
[35] C.-W. Chen, Y. W. R. Shau, and C.-P. Wu, "Analog transmission line model for simulation of systemic circulation," *IEEE Trans. Biomed. Eng.*, vol. 44, no. 1, pp. 90–94, Jan. 1997.
[36] P. Vanassche, G. Gielen, and W. Sansen, "Symbolic modeling of periodically time-varying systems using harmonic transfer matrices," *IEEE Trans. Comput.-Aided Des. Integr. Circuits Syst.*, vol. 21, no. 9, pp. 1011–1024, Sep. 2002.
[37] J. T. Ottesen, M. S. Olufsen, and J. Larsen, *Applied Mathematical Models in Human Physiology* (SIAM Monographs on Mathematical Modeling and Computation Series). Philadelphia, PA, USA: SIAM, 2004.
[38] T. Nakano, T. Suda, M. Moore, R. Egashira, A. Enomoto, and K. Arima, "Molecular communication for nanomachines using intercellular calcium signaling," in *Proc. 5th IEEE Conf. Nanotechnol.*, Nagoya, Japan, Jul. 2005, pp. 478–481.
[39] A. O. Bicen, I. F. Akyildiz, S. Balasubramaniam, and Y. Koucheryavy, "Linear channel modeling and error analysis for intra/inter-cellular Ca^{2+} molecular communication," *IEEE Trans. Nanobiosci.*, vol. 15, no. 5, pp. 488–498, Jul. 2016.
[40] M. J. Berridge, M. D. Bootman, and H. L. Roderick, "Calcium signalling: Dynamics, homeostasis and remodelling," *Nature Rev. Mol. Cell Biol.*, vol. 4, no. 7, pp. 517–529, Jul. 2003.
[41] S. Schuster, M. Marhl, and T. Höfer, "Modelling of simple and complex calcium oscillations," *Eur. J. Biochem.*, vol. 269, no. 5, pp. 1333–1355, Mar. 2002.
[42] R. F. Probstein, *Physicochemical Hydrodynamics*. Hoboken, NJ, USA: Wiley, 1994.
[43] T. Nakano and J.-Q. Liu, "Design and analysis of molecular relay channels: An information theoretic approach," *IEEE Trans. Nanobiosci.*, vol. 9, no. 3, pp. 213–221, Sep. 2010.
[44] M. T. Barros, S. Balasubramaniam, and B. Jennings, "Comparative end-to-end analysis of Ca^{2+}-signaling-based molecular communication in biological tissues," *IEEE Trans. Commun.*, vol. 63, no. 12, pp. 5128–5142, Dec. 2015.
[45] A. Korngreen, V. Gold'shtein, and Z. Priel, "A realistic model of biphasic calcium transients in electrically nonexcitable cells," *Biophys. J.*, vol. 73, no. 2, pp. 659–673, Aug. 1997.
[46] T. Höfer, L. Venance, and C. Giaume, "Control and plasticity of intercellular calcium waves in astrocytes: A modeling approach," *J. Neurosci.*, vol. 22, no. 12, pp. 4850–4859, Jun. 2002.
[47] D. Malak and O. B. Akan, "Communication theoretical understanding of intra-body nervous nanonetworks," *IEEE Commun. Mag.*, vol. 52, no. 4, pp. 129–135, Apr. 2004.
[48] D. Malak and O. B. Akan, "A communication theoretical analysis of synaptic multiple-access channel in hippocampal-cortical neurons," *IEEE Trans. Commun.*, vol. 61, no. 6, pp. 2457–2467, Jun. 2013.
[49] E. Balevi and O. B. Akan, "A physical channel model for nanoscale neuro-spike communications," *IEEE Trans. Commun.*, vol. 61, no. 3, pp. 1178–1187, Mar. 2013.
[50] H. Ramezani and O. B. Akan, "Impacts of spike shape variations on synaptic communication," *IEEE Trans. Nanobiosci.*, vol. 17, no. 3, pp. 260–271, Jul. 2018.
[51] M. Veletić, P. A. Floor, Y. Chahibi, and I. Balasingham, "On the upper bound of the information capacity in neuronal synapses," *IEEE Trans. Commun.*, vol. 64, no. 12, pp. 5025–5036, Dec. 2016.
[52] B. L. Bassler, "Small talk: Cell-to-cell communication in bacteria," *Cell*, vol. 109, pp. 421–424, May 2002.
[53] B. L. Bassler, "How bacteria talk to each other: Regulation of gene expression by quorum sensing," *Current Opinion Microbiol.*, vol. 2, no. 6, pp. 582–587, Dec. 1999.
[54] S. Abadal and I. F. Akyildiz, "Automata modeling of quorum sensing for nanocommunication networks," *Nano Commun. Netw.*, vol. 2, no. 1, pp. 74–83, Mar. 2011.
[55] A. O. Bicen, C. M. Austin, I. F. Akyildiz, and C. R. Forest, "Efficient sampling of bacterial signal transduction for detection of pulse-amplitude modulated molecular signals," *IEEE Trans. Biomed. Circuits Syst.*, vol. 9, no. 4, pp. 505–517, Aug. 2015.
[56] B. Krishnaswamy *et al.*, "Time-elapse communication: Bacterial communication on a microfluidic chip," *IEEE Trans. Commun.*, vol. 61, no. 12, pp. 5139–5151, Dec. 2013.
[57] B. D. Unluturk and I. F. Akyildiz, "An end-to-end model of plant pheromone channel for long range molecular communication," *IEEE Trans. Nanobiosci.*, vol. 16, no. 1, pp. 11–20, Jan. 2017.
[58] I. F. Akyildiz, F. Fekri, R. Sivakumar, C. R. Forest, and B. K. Hammer, "Monaco: Fundamentals of molecular nano-communication networks," *IEEE Wireless Commun.*, vol. 19, no. 5, pp. 12–18, Oct. 2012.
[59] A. Einolghozati, M. Sardari, F. Fekri, "Design and analysis of wireless communication systems using diffusion-based molecular communication among bacteria," *IEEE Trans. Wireless Commun.*, vol. 12, no. 12, pp. 6096–6105, Dec. 2013.
[60] T. Khan, B. A. Bilgin, and O. B. Akan, "Diffusion-based model for synaptic molecular communication channel," *IEEE Trans. Nanobiosci.*, vol. 16, no. 4, pp. 299–308, Jun. 2017.
[61] H. Ramezani and O. B. Akan, "Information capacity of vesicle release in neuro-spike communication," *IEEE Commun. Lett.*, vol. 22, no. 1, pp. 41–44, Jan. 2018.
[62] D. Kilinc and O. B. Akan, "An information theoretical analysis of nanoscale molecular gap junction communication channel between cardiomyocytes," *IEEE Trans. Nanotechnol.*, vol. 12, no. 2, pp. 129–136, Mar. 2013.
[63] J. Müller, C. Kuttler, and B. A. Hense, "Sensitivity of the quorum sensing system is achieved by low pass filtering," *Biol. Syst.*, vol. 92, no. 1, pp. 76–81, Apr. 2008.
[64] P. Melke, P. Sahlin, A. Levchenko, and H. Jönsson, "A cell-based model for quorum sensing in heterogeneous bacterial colonies," *PLoS Comput. Biol.*, vol. 6, no. 6, pp. e1000819-1–e1000819-13, Jun. 2010.
[65] L. C. Cobo and I. F. Akyildiz, "Bacteria-based communication in nanonetworks," *Nano Commun. Netw.*, vol. 1, no. 4, pp. 244–256, 2010.
[66] S. Balasubramaniam and P. Lio', "Multi-hop conjugation based bacteria nanonetworks," *IEEE Trans. Nanobiosci.*, vol. 12, no. 1, pp. 47–59, Mar. 2013.
[67] M. Gregori and I. F. Akyildiz, "A new nanonetwork architecture using flagellated bacteria and catalytic nanomotors," *IEEE J. Sel. Areas Commun.*, vol. 28, no. 4, pp. 612–619, May 2010.
[68] B. D. Unluturk, S. Balasubramaniam, and I. F. Akyildiz, "The impact of social behavior on the attenuation and delay of bacterial nanonetworks," *IEEE Trans. Nanobiosci.*, vol. 15, no. 8, pp. 959–969, Dec. 2016.
[69] N. Goldman *et al.*, "Towards practical, high-capacity, low-maintenance information storage in synthesized DNA," *Nature*, vol. 494, no. 7435, pp. 77–80, Feb. 2013.
[70] M. Gao, "Free Ornstein–Uhlenbeck processes," *J. Math. Anal. Appl.*, vol. 322, no. 1, pp. 177–192, 2006.
[71] J. Beeg, S. Klumpp, R. Dimova, R. S. Gracià, E. Unger, and R. Lipowsky, "Transport of beads by several kinesin motors," *Biophys. J.*, vol. 94, no. 2, pp. 532–541, Jan. 2008.
[72] Y. Chahibi, I. F. Akyildiz, and I. Balasingham, "Propagation modeling and analysis of molecular motors in molecular communication," *IEEE Trans. Nanobiosci.*, vol. 15, no. 8, pp. 917–927, Dec. 2016.
[73] M. Moore *et al.*, "A design of a molecular communication system for nanomachines using molecular motors," in *Proc. 4th Annu. IEEE Int. Conf. Pervasive Comput. Commun. Workshops*, Mar. 2006, pp. 553–559
[74] A. O. Bicen and I. F. Akyildiz, "Interference modeling and capacity analysis for microfluidic molecular communication channels," *IEEE Trans. Nanotechnol.*, vol. 14, no. 3, pp. 570–579, May 2015.
[75] A. O. Bicen, J. J. Lehtomäki, and I. F. Akyildiz, "Shannon meets fick on the microfluidic channel: Diffusion limit to sum broadcast capacity for molecular communication," *IEEE Trans. Nanobiosci.*, vol. 17, no. 1, pp. 88–94, Jan. 2018.

[76] A. O. Bicen and I. F. Akyildiz, "System-theoretic analysis and least-squares design of microfluidic channels for flow-induced molecular communication," *IEEE Trans. Signal Process.*, vol. 61, no. 20, pp. 5000–5013, Oct. 2013.
[77] M. J. Moore, T. Suda, and K. Oiwa, "Molecular communication: Modeling noise effects on information rate," *IEEE Trans. Nanobiosci.*, vol. 8, no. 2, pp. 169–180, Jun. 2009.
[78] S. A. Wirdatmadja, D. Moltchanov, S. Balasubramaniam, and Y. Koucheryavy, "Microfluidic system protocols for integrated on-chip communications and cooling," *IEEE Access*, vol. 5, pp. 2417–2429, 2017.
[79] M. Kuscu and O. B. Akan, "Modeling convection-diffusion-reaction systems for microfluidic molecular communications with surface-based receivers in Internet of Bio-Nano Things," *PLoS ONE*, vol. 13, no. 2, Feb. 2018, Art. no. e0192202.
[80] G. M. Whitesides, "The origins and the future of microfluidics," *Nature*, vol. 442, no. 7101, pp. 368–373, Jul. 2006.
[81] D. Mark, S. Haeberle, G. Roth, F. von Stetten, and R. Zengerle, "Microfluidic lab-on-a-chip platforms: Requirements, characteristics and applications," *Chem. Soc. Rev.*, vol. 39, 2010.
[82] S. Hiyama, Y. Moritani, R. Gojo, S. Takeuchi, and K. Sutoh, "Biomolecular-motor-based autonomous delivery of lipid vesicles as nano- or microscale reactors on a chip," *Lab Chip*, vol. 10, no. 20, pp. 2741–2748, 2010.
[83] V. Jamali, N. Farsad, R. Schober, and A. Goldsmith, "Non-coherent detection for diffusive molecular communication systems," *IEEE Trans. Commun.*, vol. 66, no. 6, pp. 2515–2531, Jun. 2018.

ABOUT THE AUTHORS

Ian F. Akyildiz (Fellow, IEEE) received the M.S. and Ph.D. degrees in computer engineering from the University of Erlangen–Nuremberg, Erlangen, Germany, in 1978, 1981, and 1984, respectively.

He is currently the Ken Byers Chair Professor of telecommunications with the School of Electrical and Computer Engineering, Georgia Institute of Technology, Atlanta, GA, USA, where he is also the Director of the Broadband Wireless Networking Laboratory and the Chair of the Telecommunication Group. His current research interests include terahertz communications, nanonetworks, Internet of Nanothings, Internet of Bio-Nano Things, 5G/6G wireless systems, Internet of Space Things/CUBESATs, and wireless sensor networks in challenged environments, on which he has authored or coauthored more than 400 articles in prestigious journals and conferences. According to Google Scholar, his h-index is 117 and the total number of citations of his papers is more than 107K as of 2019.

Dr. Akyildiz has been a Fellow of ACM since 1997. He was a recipient of numerous awards from IEEE and ACM.

Massimiliano Pierobon (Member, IEEE) received the Ph.D. degree in electrical and computer engineering from the Georgia Institute of Technology, Atlanta, GA, USA, in 2013.

Since 2013, he has been an Assistant Professor with the Department of Computer Science and Engineering, University of Nebraska–Lincoln (UNL), Lincoln, NE, USA, where he also holds a courtesy appointment with the Department of Biochemistry. Since 2016, he has been a Faculty Mentor with the iGEM Team, UNL. He is currently the Principal Investigator of multiple NSF projects in the field of molecular communication (MC) applied to biological systems. His current research interests include MC theory, nanonetworks, intrabody networks, communication engineering applied to synthetic biology, and the Internet of Bio-Nano Things.

Dr. Pierobon has been the Coeditor-in-Chief of *Nano Communication Networks* (Elsevier) since 2017, and an Associate Editor of the IEEE TRANSACTIONS ON COMMUNICATIONS since 2013. He was a recipient of the 2017 IEEE INFOCOM Best Paper Runner-up Award and the IEEE GLOBECOM 2017 Best Paper Award.

Sasitharan Balasubramaniam (Senior Member, IEEE) received the B.E. degree in electrical and electronic engineering from the University of Queensland, Brisbane, QLD, Australia, in 1998, the M.E. in computer and communication engineering from the Queensland University of Technology, Brisbane, in 1999, and the Ph.D. degree from the University of Queensland, in 2005.

He is currently an Academy of Finland Research Fellow with the Tampere University of Technology, Tampere, Finland. He is also the Director of research with the Telecommunication Software and Systems Group, Waterford Institute of Technology, Waterford, Ireland. He has authored or coauthored more than 100 articles in various journals and conferences, and actively participates in a number of technical program committees for various conferences. His current research interests include bioinspired communication networks and molecular communications.

Dr. Balasubramaniam was the TPC Co-Chair in 2014 and the General Chair in 2015. He is currently on the Steering Board Committee of ACM NANOCOM, which he co-founded. In 2018, he was the IEEE Nanotechnology Council Distinguished Lecturer. He was an Associate Editor of the IEEE INTERNET OF THINGS JOURNAL. He is currently an Associate Editor of the IEEE LETTERS OF THE COMPUTER SOCIETY, *Elsevier Nano Communication Networks*, and *Elsevier Digital Communication and Networks*.